

Modeling Water Resource Systems under Climate Change: IGSM-WRS

Kenneth Strzepek, Adam Schlosser, Arthur Gueneau, Xiang Gao,
Élodie Blanc, Charles Fant, Bilhuda Rasheed and Henry D. Jacoby



Report No. 236
December 2012

The MIT Joint Program on the Science and Policy of Global Change is an organization for research, independent policy analysis, and public education in global environmental change. It seeks to provide leadership in understanding scientific, economic, and ecological aspects of this difficult issue, and combining them into policy assessments that serve the needs of ongoing national and international discussions. To this end, the Program brings together an interdisciplinary group from two established research centers at MIT: the Center for Global Change Science (CGCS) and the Center for Energy and Environmental Policy Research (CEEPR). These two centers bridge many key areas of the needed intellectual work, and additional essential areas are covered by other MIT departments, by collaboration with the Ecosystems Center of the Marine Biology Laboratory (MBL) at Woods Hole, and by short- and long-term visitors to the Program. The Program involves sponsorship and active participation by industry, government, and non-profit organizations.

To inform processes of policy development and implementation, climate change research needs to focus on improving the prediction of those variables that are most relevant to economic, social, and environmental effects. In turn, the greenhouse gas and atmospheric aerosol assumptions underlying climate analysis need to be related to the economic, technological, and political forces that drive emissions, and to the results of international agreements and mitigation. Further, assessments of possible societal and ecosystem impacts, and analysis of mitigation strategies, need to be based on realistic evaluation of the uncertainties of climate science.

This report is one of a series intended to communicate research results and improve public understanding of climate issues, thereby contributing to informed debate about the climate issue, the uncertainties, and the economic and social implications of policy alternatives. Titles in the Report Series to date are listed on the inside back cover.


Ronald G. Prinn and John M. Reilly
Program Co-Directors

For more information, please contact the Joint Program Office

Postal Address: Joint Program on the Science and Policy of Global Change
77 Massachusetts Avenue
MIT E19-411
Cambridge MA 02139-4307 (USA)

Location: 400 Main Street, Cambridge
Building E19, Room 411
Massachusetts Institute of Technology

Access: Phone: +1.617. 253.7492
Fax: +1.617.253.9845
E-mail: globalchange@mit.edu
Web site: <http://globalchange.mit.edu/>

 Printed on recycled paper

Modeling Water Resource Systems under Climate Change: IGSM-WRS
 Kenneth Strzepek^{*†}, Adam Schlosser^{*}, Arthur Gueneau^{*}, Xiang Gao^{*}, Élodie Blanc^{*},
 Charles Fant^{*}, Bilhuda Rasheed^{*} and Henry D. Jacoby^{*}

Abstract

Through the integration of a Water Resource System (WRS) component, the MIT Integrated Global System Model (IGSM) framework has been enhanced to study the effects of climate change on managed water-resource systems. Development of the WRS involves the downscaling of temperature and precipitation from the zonal representation of the IGSM to regional (latitude-longitude) scale, and the translation of the resulting surface hydrology to runoff at the scale of river basins, referred to as Assessment Sub-Regions (ASRs). The model of water supply is combined with analysis of water use in agricultural and non-agricultural sectors and with a model of water system management that allocates water among uses and over time and routes water among ASRs. Results of the IGSM-WRS framework include measures of water adequacy and ways it is influenced by climate change. Here we document the design of WRS and its linkage to other components of the IGSM, and present tests of consistency of model simulations with the historical record.

Contents

1. MODELING FRAMEWORK	2
1.1 Model Components	2
1.2 Application at the Global Scale	4
2. HYDROLOGY AND RUNOFF AT THE ASR SCALE	5
2.1 Spatial Transformation of IGSM Climate	6
2.2 Hydrology and Runoff Projections	8
2.2.1 Land-Surface Hydrology	9
2.2.2 CLM-Based Flow at the ASR Scale	10
2.2.3 Bias Correction of ASR Natural Runoff	11
3. WATER SYSTEM MANAGEMENT	16
3.1 Water Supply	16
3.1.1 Surface Water Movements	16
3.1.2 Groundwater	16
3.1.3 Desalination	17
3.1.4 Total Available Water	18
3.2 Water Requirements	18
3.2.1 Irrigation	18
3.2.2 Non-Irrigation	19
3.2.3 Total Water Requirement	19
3.2.4 Environmental Flow Requirement	19
3.3 Supply-Demand Balance	19
3.3.1 The ASR Water Balance and Virtual Reservoir Operation	19
3.3.2 Water Allocation	20
4. AGRICULTURAL WATER USE	21
4.1 Irrigation Water Requirement	21
4.1.1 Potential Evaporation	21
4.1.2 Water Consumption at the Root	25
4.1.3 Delivery Efficiencies	25
4.2 Livestock Water Use	26
5. NON-AGRICULTURAL WATER USES	26

^{*} Joint Program on the Science and Policy of Global Change, Massachusetts Institute of Technology, Cambridge, MA, USA.

[†] Corresponding Author: Kenneth Strzepek (Email: Strzepek@mit.edu).

5.1 Municipal Water Use.....	26
5.2 Industrial Water Use.....	27
6. ASSESSMENT OF MODEL PERFORMANCE	27
6.1 Results at the Global Scale	28
6.1.1 Runoff.....	28
6.1.2 Irrigation Requirements by Crop	29
6.1.3 Water Requirements by Sector	29
6.2 Results at the Basin Scale.....	36
6.2.1 Runoff.....	36
6.2.2 Water Requirements	37
6.3 Water Stress.....	38
6.3.1 Global Water Stress.....	39
6.3.2 ASR Level Water Stress	41
7. SUMMARY AND APPLICATIONS.....	42
8. REFERENCES	43
APPENDIX.....	47

1. MODELING FRAMEWORK

1.1 Model Components

Changing climate and growing population threaten to increase stress on available fresh water, with implications for irrigation, energy production and other uses and, in extreme cases, the stability of nations. The MIT Integrated Global System Model (IGSM) (Sokolov *et al.*, 2007) is designed to study global climate change and its social and environmental consequences, quantifying the associated uncertainties, and assess the cost and effectiveness of policies proposed to mitigate the risk. To support assessment of these issues the IGSM has been expanded to include a Water Resource System (WRS) component that integrates the managed aspect of the hydrologic cycle. The resulting IGSM-WRS framework includes:

- (1) Water supply: the collection, storage and diversion of natural surface water and groundwater;
- (2) Water requirements: the withdrawal, consumption and flow management of water for economic and environmental purposes; and
- (3) The supply/requirement balance at river basin scale and measures of water scarcity, particularly its effects on agriculture.

In this report we describe the IGSM-WRS framework and demonstrate its performance in a backcast of the 20th century. Parallel efforts apply the model to projections at the global scale (Schlosser *et al.*, 2012), and to the United States (Blanc *et al.*, 2012).

The WRS component of the IGSM framework draws on two lines of research on global water systems: one at the University of Colorado (CU) on the impacts of climate change upon hydrological systems, and another by the International Food Policy Research Institute (IFPRI), on global food and agricultural systems. Work at CU began with a national-level assessment of water resources supply-demand balances for the United Nations Comprehensive Fresh Water

Assessment (Raskin *et al.*, 1997). This national-level analysis was extended and incorporated in the Stockholm Environment Institute’s Polestar model (Raskin *et al.*, 1998), and included by the World Water Council in an analysis for its World Water Vision 2000 (Gangopadhyay *et al.*, 2001; Cosgrove and Rijsberman, 2000). Concerns about food security and trade led to an effort by IFPRI and partner collaborators to develop the IMPACT-WATER model, which integrates a global partial-equilibrium agricultural sector model, IMPACT, with a water simulation module that balances water availability and demands among economic sectors at global and regional scales (Rosegrant, 2008).

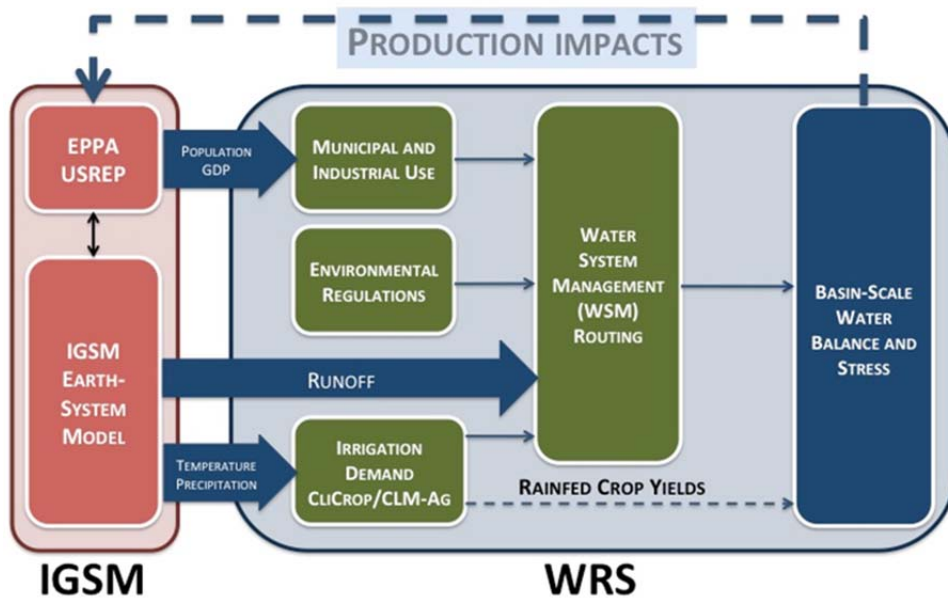


Figure 1. Schematic of IGSM-WRS model illustrating the connections between the economic and climate components of the IGSM framework and the WRS component. Solid arrows represent connections utilized in this research; dashed arrows represent WRS links under development.

Figure 1 summarizes how the WRS is integrated within the IGSM framework. Given a scenario of global climate policy, the IGSM provides the WRS with economic drivers, relevant climate variables, and inputs to the estimation of runoff. WRS combines these inputs with estimates of water requirements and simulates the operation of the water management system to assess the ability to meet these requirements at the river basin level. Currently this is a one-way connection between the economic and climate components of the water system. In subsequent stages of model development the economic effects of changes in the water system will be fed back into the economic analysis, as indicated by the dashed line in Figure 1.

The economic analysis component of the IGSM is the MIT Emissions Prediction and Policy Analysis (EPPA) model (Paltsev *et al.*, 2005).¹ It provides emissions inputs to the Earth system part of the IGSM and supplies socio-economic information used in the estimation of non-agricultural water demands. Runoff is calculated by a procedure that begins with the Community Land Model (CLM) that is employed in the Global Land System (GLS) component of the IGSM's Earth System Model (Schlosser *et al.*, 2007). The IGSM's atmosphere resolves zonal and altitude variations, so the meteorological variables must be downscaled across longitude. The subsequent runoff calculation then proceeds through several steps of calibration and bias correction (Section 2). The current application employs a deterministic representation of runoff. Subsequent stages of this research will incorporate uncertainty in the climate analysis (Sokolov *et al.*, 2009; Webster *et al.*, 2012) and the future patterns (resulting from human-induced climate change) used in downscaling, applying a method developed by Schlosser *et al.*, (2012).

Runoff and water requirements are then input to a Water System Management module (WSM) developed by IFPRI (Rosengrant, 2008) which simulates the water supply and demand balance, allocating available water among competing sectors (Section 3). The Earth System component of the IGSM supplies simulated temperature, precipitation and potential evapotranspiration, which are inputs to a model of irrigation water requirements, CliCrop (Fant *et al.*, 2012), discussed in Section 4.² The estimation of non-agricultural water requirements, covered in Section 5, is based on the IMPACT-WATER framework and draws on economic data from the EPPA model. A number of indicators of water system function, such as water stress, can be computed from the runoff and water use information and from the results of the supply-demand balance and water allocation.

In Section 6 we explore aspects of the model's performance by calibrating it to the period 1954–1977 and comparing results for various output measures with observations or other constructions of basin characteristics for the period 1981–2000. Section 7 reviews the results of the model development and summarizes the applications of the IGSM-WRS to analysis of the effects of projected climate change.

1.2 Application at the Global Scale

We describe the application of the IGSM-WRS at the global level, disaggregated into 282 Assessment Sub-Regions (ASRs).³ The ASRs are based on IFPRI's IMPACT-WATER model's "food-producing units". These were created by first dividing the globe into 106 hydrologic regions or river basins (Appendix Table A2) and then by separately defining 116 economic

¹ In an application focused on the U.S. (Blanc *et al.*, 2012) results from the EPPA model are disaggregated for the U.S. by a regional energy model.

² The IGSM-WRS also supports estimation of both rainfed and irrigated agricultural production, though this feature is not used in the application documented here.

³ Use of the term ASR for the unit of water analysis originates in the U.S. In application focused on the U. S. (Blanc *et al.*, 2012) a 99-basin definition is used, and because of superior data availability in the U.S., other models of the non-agricultural sectors are implemented.

regions (mainly nations), which identify the political boundaries of management policy. The selection and scale of these regions seeks to isolate the most important river basins and countries in term of water use, especially for irrigation and energy purposes, and the 282 ASRs are then defined by their intersection (Appendix Table A1). This procedure results in some international river basins being spread over several ASRs (e.g., The Indus is divided into three ASRs and the Niger is represented in nine ASRs). On the other hand many rivers basins are located within a single economic region (e.g., the Missouri Basin in the U.S.)

Figure 2 displays the ASRs, with color-coding showing their relation to the 16 region disaggregation of the EPPA model. A list of ASRs detailing their relation to national boundaries and EPPA regions is provided in the Appendix. China, India and the United States, which produce an aggregate 60% of the world’s cereal grains, have the highest level of sub-national disaggregation, being divided into 9, 13 and 14 major river basins, respectively.

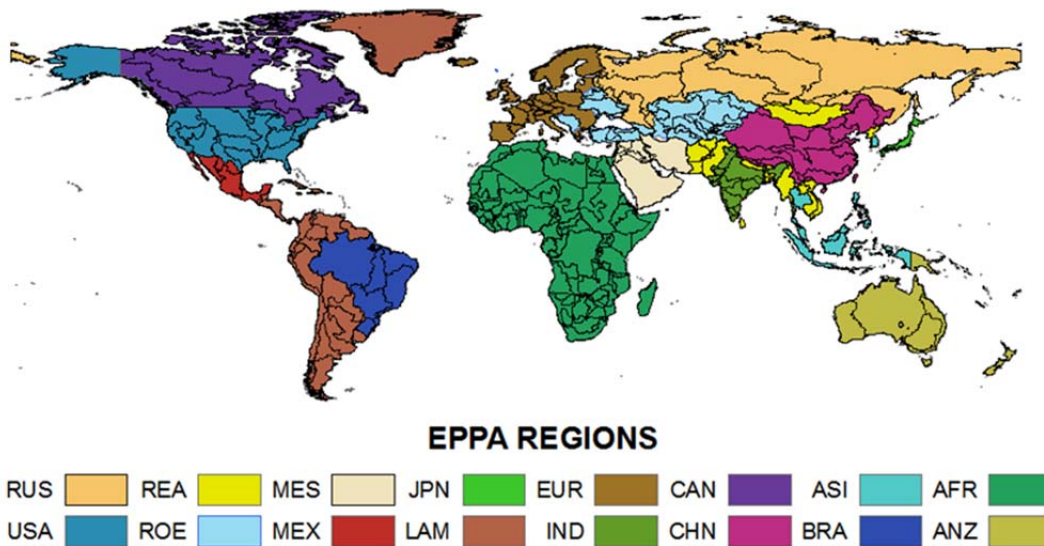


Figure 2. The 282 water Assessment Sub-Regions (ASRs) of the IGSM-WRS at global scale colored by EPPA Region. A detailed listing of the ASRs and their mapping to EPPA regions is provided in the Appendix.

2. HYDROLOGY AND RUNOFF AT THE ASR SCALE

The IGSM’s Climate and Earth system component employs a numerically efficient 2-dimensional (latitude zones and altitude) modeling approach, which makes it possible to develop large ensembles of climate predictions for purposes of studying uncertainty in the water resource effects of climate change. The downscaling from 2-D climate to flows at the basin level involves a number of steps: 2-D to 3-D climate, hydrology and runoff projection, and a correction for bias common to the simulation of river flows in climate models.

2.1 Spatial Transformation of IGSM Climate

A procedure developed by Schlosser *et al.* (2012) is applied to translate the zonal (latitude mean) field of any state or flux variable of the IGSM, \bar{V}_y^{IGSM} , to longitudinal detail:

$$V_{x,y}^{IGSM} = C_{x,y} \bar{V}_y^{IGSM} \quad (1)$$

where $C_{x,y}$ is a transformation coefficient that corresponds to the longitudinal point (x) along any given latitude (y) and maps \bar{V}_y^{IGSM} to its corresponding longitudinal value, $V_{x,y}^{IGSM}$. While this transformation can apply, in principle, to any state or flux quantity, here the variables providing the links between the IGSM and WRS are surface-air temperature (T) and precipitation (P).

As described in Schlosser *et al.* (2012), for the historical period we calculate the monthly climatology of $C_{x,y}$ using observational data sets of the Climate Research Unit (CRU) (Jones *et al.*, 1999) and the Global Precipitation Climatology Project (GPCP) of Adler *et al.* (2007), for the T and P estimates, respectively. Each of these observational data sets is provided at monthly timesteps, and we build the $C_{x,y}$ climatologies accordingly. We then employ the calculated $C_{x,y}$ coefficients in Equation 1 with an IGSM simulation covering the corresponding observational record.

We can evaluate the downscaled \bar{V}_y^{IGSM} patterns by the spatial (i.e. pattern) correlation with observations for precipitation (**Figure 3**). For the period 1981–2000 we find spatial consistency between the downscaled IGSM seasonal means and observations, with correlations of 0.992 for December, January and February (DJF) and 0.987 for June, July and August (JJA). Strong spatial consistency also is found for surface air temperature (not shown).

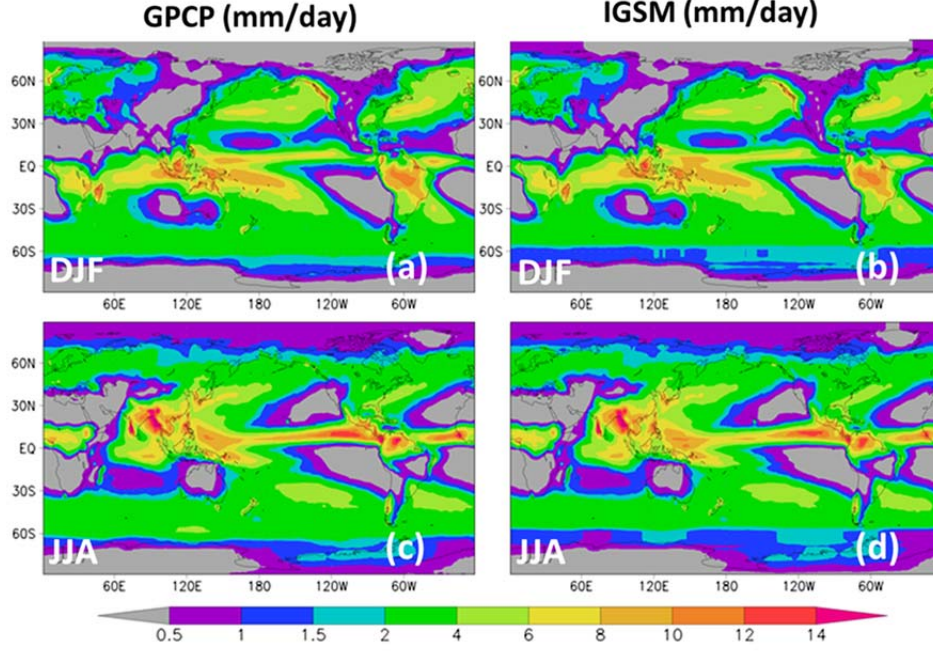


Figure 3. Shown are winter (DJF) and summer (JJA) average precipitation (1981 to 2000) comparing observations from the Global Precipitation Climatology Project (GPCP) (Adler *et al.* 2007)(a) and (c) with the IGSM downscaled precipitation based on Schlosser *et al.* (2012)(b) and (d).

When applying this framework to projections of climate change, the associated shifts and/or amplification of the $C_{x,y}$ patterns can be calculated for any climate model to take account of its projected change in longitudinal distribution over time in response to changing climate. Analytically, the procedure is a Taylor expansion of the form:

$$V_{x,y}^{IGSM}(\Delta T_{Global}) = C_{x,y}|_{t_0} \bar{V}_y^{IGSM} + \left[\frac{dC_{x,y}}{dT_{Global}} \Delta T_{Global} \right] \bar{V}_y^{IGSM} \quad (2)$$

The first term on the right-hand side of the Equation is the transformation coefficient evaluated at a reference historical time period (t_0) based on observations. In the second term, $\frac{dC_{xy}}{dT_{Global}}$ is the pattern-change kernel estimated from a climate model (see Schlosser *et al.*, 2012 for details), which employs climate model results from the CMIP3 experiments (Meehl *et al.*, 2007) in support of the IPCC 4th Assessment Report. Numerically, the pattern-change kernel quantifies the shift in $C_{x,y}$ per unit change in global temperature (ΔT_{Global}). In climate change projections these transformation patterns evolve over time as a result of the IGSM's projected global temperature change (from the zonal model). Schlosser *et al.* (2012) present a comprehensive evaluation of the application of Equation 2 with every climate model from CMIP3.

2.2 Hydrology and Runoff Projections

The IGSM-WRS requires monthly runoff of natural flows—i.e. streamflows without human intervention. Unfortunately, natural flow data are scarce because few series cover the period before intensive infrastructure development⁴. Thus natural flow must be estimated using observed flow and data on human uses augmented by climate records and hydrologic modeling. Applying simulated climate variables from the IGSM downscaling methodology described above, natural flows at the ASR level are generated in a two-step process.

First, the downscaled climate is input to the IGSM GLS component, which uses the Community Land Model (CLM) to generate raw natural flow. For reasons of scale, data and model structure, CLM simulates historical raw natural flows for some ASRs that differ from observations: in that they follow the climate signal but display a wetting or drying bias.

Second, a bias-correction technique is applied that maintains the climate signal and runoff variability from the IGSM but adjusts the simulation to replicate the historical natural flow.

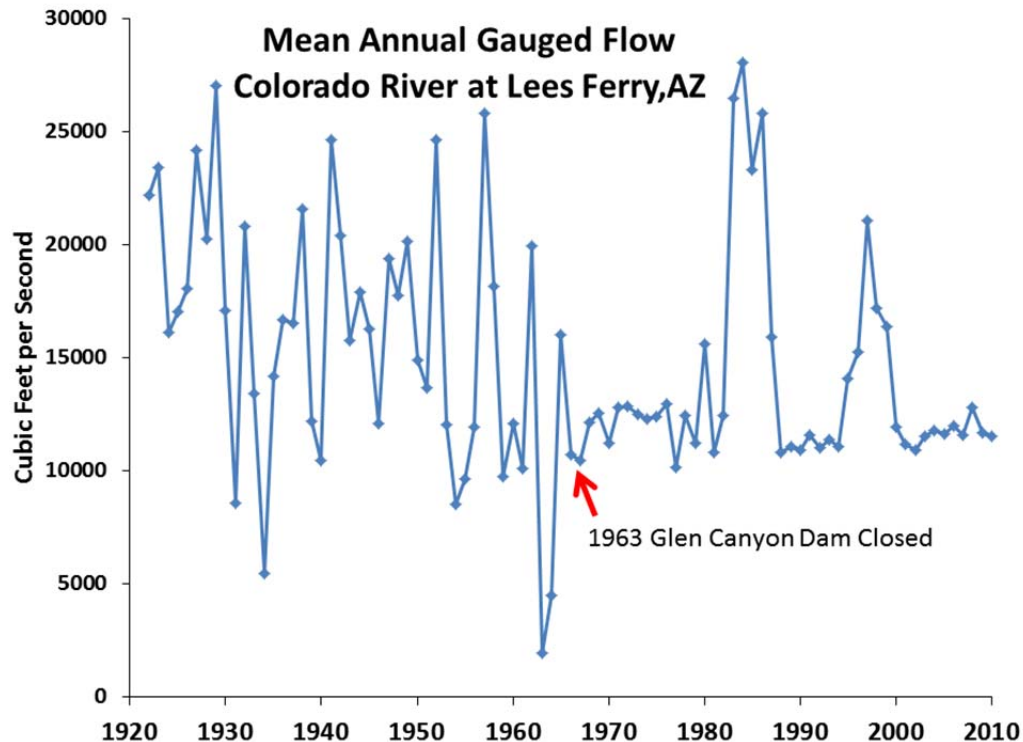


Figure 4. Annual time series of gauged Colorado River flow at Lees Ferry, Arizona, downstream of the Glen Canyon Dam and Lake Powell from 1922 to 2010. Lake Powell started filling in 1963 thus the record from 1922 up to 1963 represents Natural Flow while the record after 1962 represent managed flows (source: USGS, 2012, <http://www.waterdata.usgs.gov/az/nwis/uv?09380000>).

⁴ Figure 4 illustrates the difference between managed and natural flow with a chart of the gauged flow at Lees Ferry, Arizona—downstream of the Glen Canyon Dam and Lake Powell.

2.2.1 Land-Surface Hydrology

Within the IGSM framework, CLM (Oleson *et al.*, 2004; Lawrence *et al.*, 2011) describes the biogeophysics of the terrestrial environment. The modeled processes include the hydrologic cycle and surface energy budget over land as well as interactions with the atmosphere. The IGSM atmospheric model drives CLM, which calculates the surface and subsurface water and energy balances at a grid resolution commensurate with the modeled (or observed) atmospheric forcing. For this application we configure CLM with a horizontal resolution of 2° in latitude and 2.5° in longitude, illustrated in **Figure 5** for the U.S.

In calculating surface runoff, CLM represents the effects of limited infiltration of soils (i.e. Hortonian flow) as well as runoff from saturated surface conditions, and it also considers the effects of frozen soil conditions and root density on soil hydraulic conductivity. For subsurface runoff (and in general vertical soil-water flow), a discretized treatment of vadose zone and saturated flow is the main determinant of the vertical transport through the soil column (10 soil layers to a depth of approximately 3 m). In addition to the influence of gravity and soil-matric potential, drainage out of the bottom of the soil-column is influenced by the depth of the water table, which is represented separately as a bulk, unconfined aquifer whose drainage is governed by gravity-fed topography (for details see Lawrence *et al.*, 2011). When and where the water table depth rises into any of the soil column layers (i.e. water table depth less than 3 m), the overlapping soil layers are fed (by the groundwater) to saturation and excess soil-water becomes subsurface runoff.

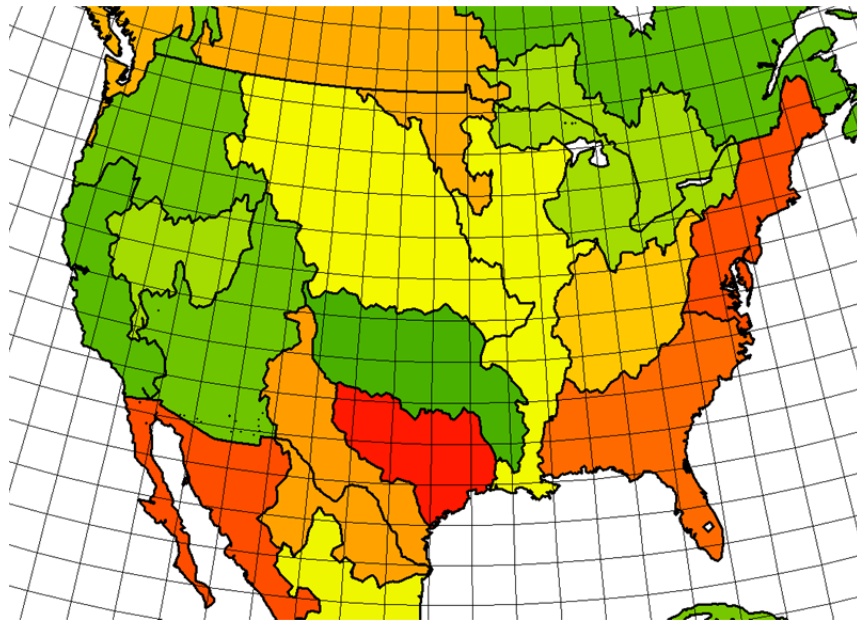


Figure 5. Illustration of the spatial scale of the IGSM/CLM grids and the Assessment Sub-Units (ASRs) of the WRS. The continental U.S. states are overlain with IGSM's 2° by 2.5° grid. Polygon areas (outlined in black and colored) are the ASRs for the global WRS configuration. CLM's adjusted runoff at each ASR is calculated by taking the area-weighted average in each CLM grid (grey rectangles).

To maintain consistency with the basin-scale resolution of the water-management scheme, we use CLM's treatment of this (unmanaged) unconfined aquifer. Currently, CLM tracks only the natural vegetated land areas, and irrigation deficits for agricultural areas are quantified by the CliCrop sub-model (Section 4). In the future, developments with CLM (Gueneau, 2012) will allow agricultural lands to be explicitly tracked within CLM, supporting a seamless link between the IGSM and WRS.

2.2.2 CLM-Based Flow at the ASR Scale

For each 2° by 2.5° grid cell CLM estimates energy and water fluxes including surface and subsurface runoff, and the two are added to produce total runoff per month in millimeters per unit area (mm/km²). Considering the surface area of each CLM grid in an ASR, illustrated in **Figure 5** for the continental U.S. (CONUS), a new time series of monthly ASR runoff is computed as the weighted average of CLM grid contributions.

While global databases of gauged flow are available (e.g., WMO, 2012) there is no corresponding database of natural flows to use in assessing the performance of this procedure at global scale. McMahon *et al.* (2007) are developing a global natural flow database based on statistical characteristics of natural flow and recreating natural flows from gauged flow, but this effort is limited in scope and not appropriate for our application. Hydrologists have taken an alternative approach using global gridded databases of climate time series and using hydrologic models to simulate natural flows. For example, Feteke *et al.* (2002) at the University of New Hampshire's Global Runoff Data Centre (GRDC) have developed a composite runoff database that combines simulated water balance model runoff estimates with monitored river discharge. This data set consists of average monthly runoff values for each cell at a 0.5° by 0.5° global land grid. A similar approach was taken by Alcamo *et al.* (2003).

Zhu *et al.* (2012) at IFPRI, have developed a global hydrological model for integrated assessment that was designed to provide natural flow at the same ASR scale as the IGSM-WRS, and they use the GPCP precipitation database and the CRU database for temperature (same as IGSM) as the monthly climate drivers for the model for the historical period 1951 to 2000. For our global scale application, we have adopted this IFPRI modeled natural flow data set, and in subsequent notation we refer to it as a Modelled Natural Flow or MNF series.

Figure 6 compares the average annual natural flow for the 282 ASRs from CLM versus IFPRI-MNF series for the period 1954 to 1977. A linear regression through the origin results in an R² of 0.84, suggesting that the CLM runoff captures the regional wetness and dryness at the large spatial scale of the ASRs. However, the slope is 1.37, meaning that the CLM generated runoff is biased downward.⁵ Milly *et al.* (2005) find that this behavior is common for land surface models global circulation models (GCM) of which CLM is one. In capturing the

⁵ The outlier in Figure 9, which will influence the regression result, is the Amazon River. If it is removed the bias is reduced but not altogether eliminated.

temporal variability and spatial signal of the climate the CLM runoff will be a good tool for analysis of relative climate change impacts, but bias correction is needed if the model is to properly balance water supply with water demand and represent water stress.

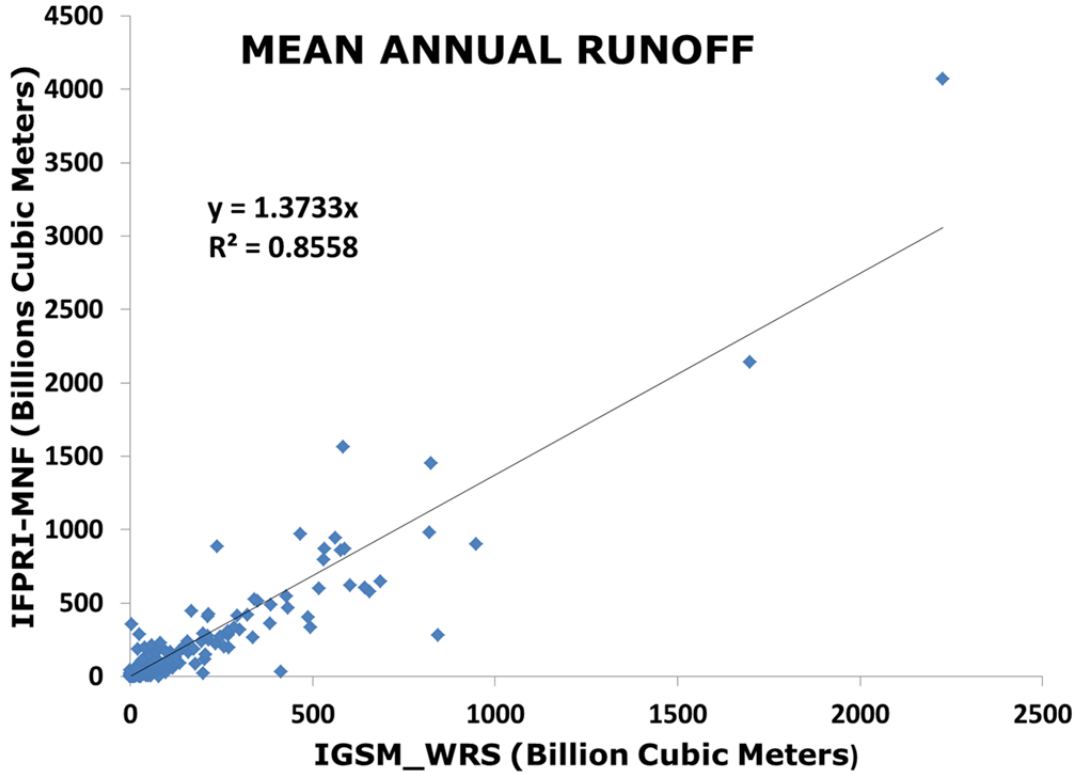


Figure 6. For mean annual runoff, 1954 to 1977. comparison of the IFPRI Modeled Natural Flow (MNF) with the WRS estimate without bias correction for 282 Assessment Sub-Regions. Statistics are for a linear regression of IFPRI MNF on WRS estimated values.

2.2.3 Bias Correction of ASR Natural Runoff

The goal of the bias correction procedure is to transform the raw CLM runoff values at the ASR level to have the same statistical properties as the IFPRI-MNF dataset for 1954 to 1977, which includes not just mean and standard deviation but also roughly the same pattern over time. We employ the Maintenance of Variance Extension (MOVE) procedure (Hirsch, 1982) to achieve this result. MOVE is commonly used to transfer streamflow information from gauged to ungauged basins, and it standardizes streamflows with two parameters: the mean and standard deviation. The method is based on the hypothesis that, for each month, the standardized flows at a site of interest, y , and an index site, x , are approximately equal.

$$\frac{Q_x - \mu_x}{\sigma_x} = \frac{Q_y - \mu_y}{\sigma_y} \quad (3)$$

A traditional standardization approach is used to produce a new standardized variable with mean zero and variance one, regardless of the probability distribution of the original flows.

To apply MOVE to IGSM-CLM runoff to estimate ASR runoff, we first calculate the mean and standard deviation for the IFPRI-MNF flows, $\mu(m)_{MNF}$ and $\sigma(m)_{MNF}$. We then transform the CLM monthly runoff, $Q_{CLM}(m,y)$, with mean, $\mu(m)_{CLM}$ and standard deviation $\sigma(m)_{CLM}$. All moments are estimated over the period 1954 to 1977, which is assumed to be stationary. The MOVE formulation can be rearranged to produce an estimate of WRS basin runoff, RUN:

$$RUN(m,y) = \mu(m)_{MNF} + \frac{\sigma(m)_{MNF}}{\sigma(m)_{CLM}} * (Q_{CLM}(m,y) - \mu(m)_{CLM}) \quad (4)$$

The Bias Correction Factor is then:

$$\frac{\sigma(m)_{MNF}}{\sigma(m)_{CLM}} \quad (5)$$

The IGSM-WRS bias-correction method uses the first two moments of the IFPRI-Modeled Natural Flow (MNF) and the IGSM-CLM simulated runoff over 1954 to 1977 for each ASR. **Figure 7** shows its performance by plotting annual global runoff from the bias-corrected IGSM-CLM simulated runoff (IGSM-WRS) with the IFPRI-MNF annual global runoff for 1954 to 1977 (**Figure 7a**). The actual annual flow sequences are not identical due to the fact that the IGSM-WRS runoff is driven by the IGSM-GCM outputs from 1954 to 1977 with historic GHG emissions and the IFPRI-MNF annual global runoff is driven by historical climate from 1954 to 1977. However, the mean global runoff for IGSM-WRS and IFPRI-MNF averaged over 1954 to 1977 are almost identical at 40,099 and 39,995 billion cubic meters, respectively. **Figure 7b** is a scatterplot of the spatial correlation of the mean annual runoff of the IGSM-WRS runoff versus the IFPRI-MNF for the 282 ASRs for the assumed stationary period 1954 to 1977. The slope of the linear regression line through the origin of 1.0034 suggests that geographical climate signals driving both series are very similar. The results presented in **Figure 7** along with additional data analysis confirm that the bias-correction procedure works well, at least as compared with this constructed data set for undisturbed flows.

The procedure is for stationary monthly stream flows, but under climate change modeled runoff exhibits monthly and seasonal non-stationaries. In some basins warming can lead to early 21st century snowmelt runoff far greater than the 20th century average for a late winter month, so the application of stationary techniques to map 21st century flow can result in erroneous estimates (e.g., Milley, *et al.*, 2008).

To handle these conditions a non-stationary extension to the MOVE technique is applied to address the issue of seasonal regime change of runoff under future climates, especially for basins affected by snowmelt. The approach uses a 10-year moving average of the index variable, CLM monthly runoff, $\mu_{CLM_MA10}(m,y)$ and develops a trend relative to the 1955 to 1977 baseline:

$$TrCLM(m,y) = \frac{\mu_{CLM_MA10}(m,y)}{\mu_{CLM}(m)} \quad (6)$$

This modification is similar to that employed by (Maurer, 2007) where the 21st century GCM trend of temperature is removed and then bias-correction is applied to the residual magnitudes to

create adjusted GCM estimates. The WRS projected runoff is then estimated based on the CLM trend and the CLM residual times the historical bias-correction factor and is expressed as:

$$RUN(m, j) = \mu(m) * TrCLM(m, j) + \frac{\sigma(m)_{MNF}}{\sigma(m)_{CLM}} * (Q_{CLM(m, j)} - \mu_{CLM_MA10(m, j)}) \quad (7)$$

Figure 8 shows a diagram of the non-stationary MOVE technique.

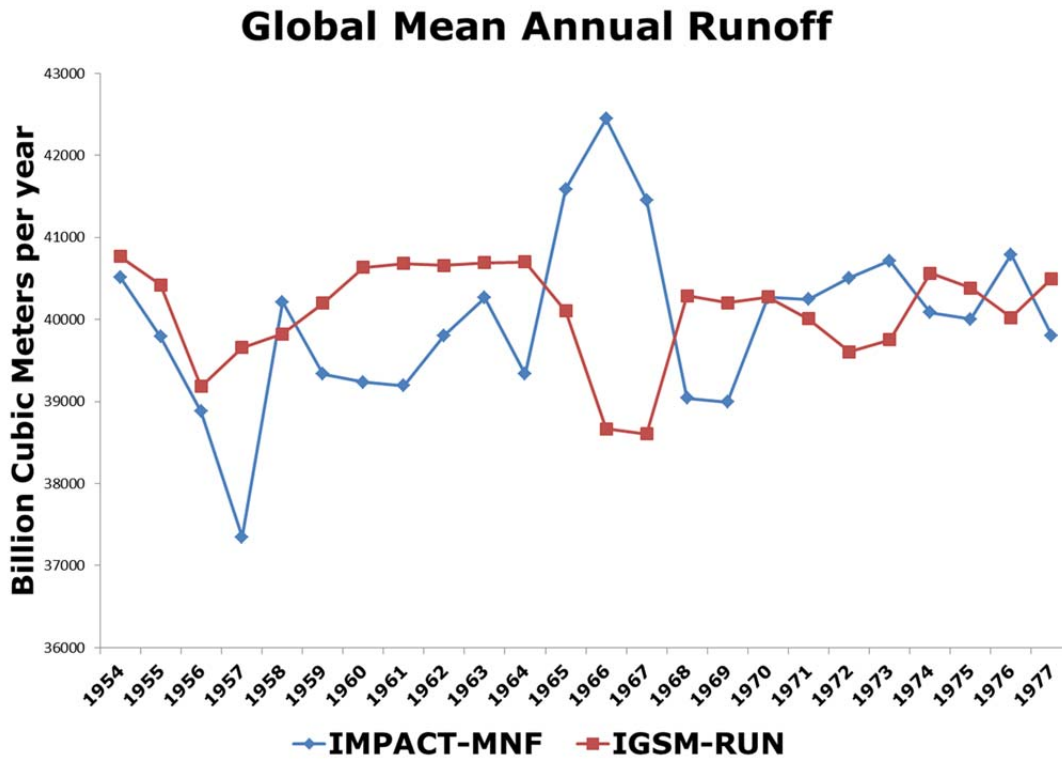


Figure 7a. Comparison of global annual runoff between the IGSM-WRS biased-corrected flow and the IFPRI-Modeled Natural Flow (MNF) over 1954 to 1977 for the summation over all the 282 global ASRs . The IGSM-WRS bias-correction method uses the first two moments of the IFPRI-Modeled Natural Flow (MNF) averaged over 1954 to 1977 for each ASR.

Mean Annual Runoff 1954-1977

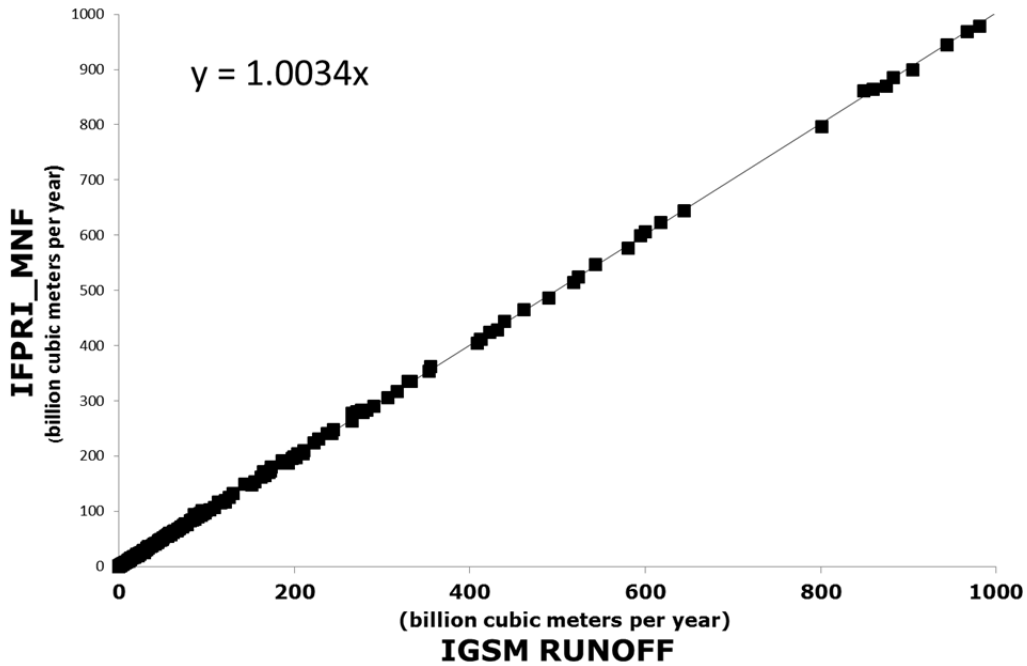


Figure 7b. Comparison of mean annual flow between the IGSM-WRS bias-corrected flow averaged over 1954 to 1977 (x-axis) and the IFPRI-Modeled Natural Flow (MNF) averaged over 1954 to 1977 (y-axis) for the 282 global ASRs. The IGSM-WRS bias-correction method uses the first two moments of the IFPRI-Modeled Natural Flow (MNF) averaged over 1954 to 1977 for each ASR.

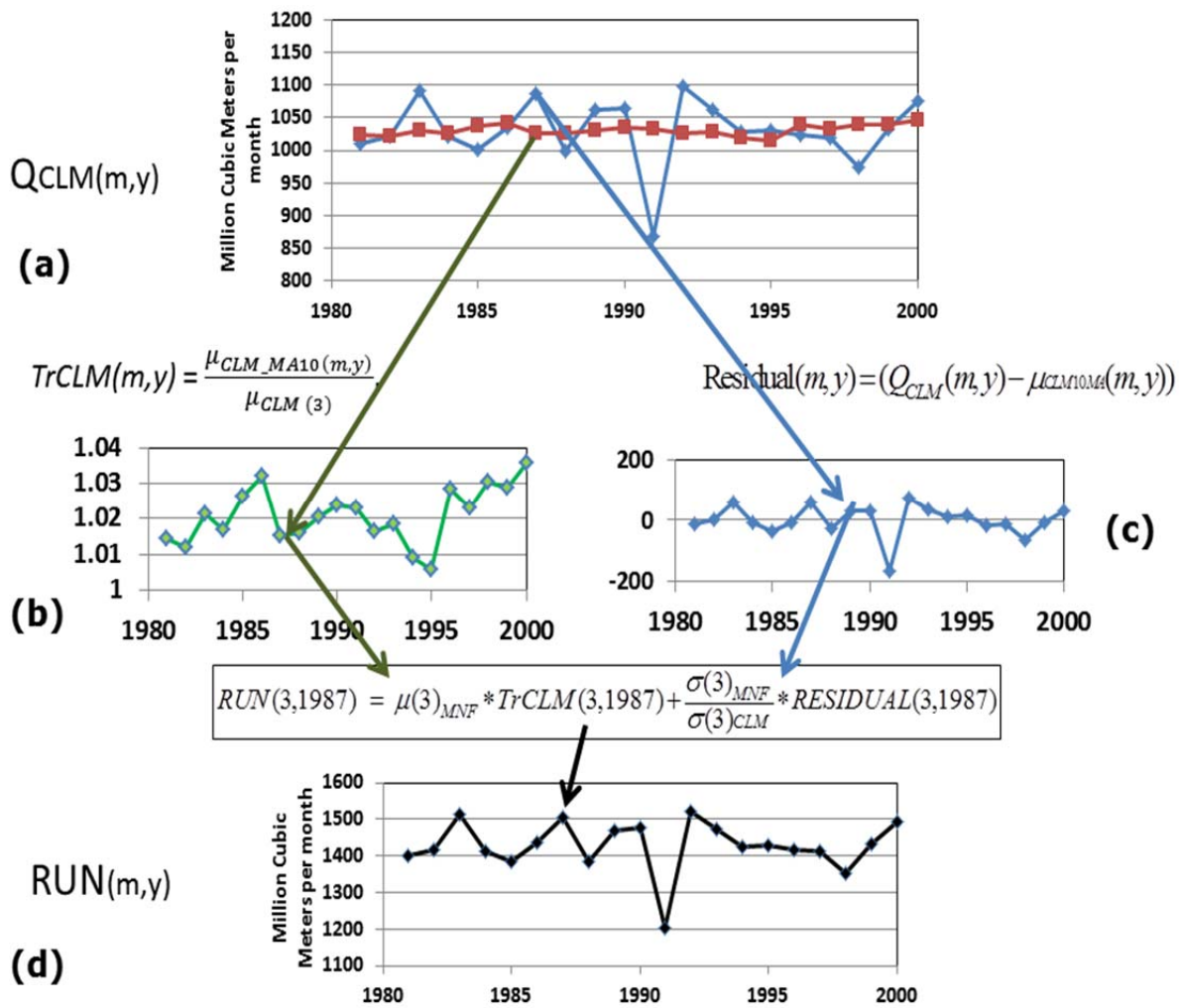


Figure 8. Illustration for a representative ASR and a representative month, 3, of the CLM runoff bias-correction methodology (the non-stationary MOVE-12 technique) used to generate IGSM-CLM runoff for the post calibration period, 1978 to 2000. Shown are the: (a) 23 yearly values of MNF from CLM with the 10-year moving average plotted on top; (b) ratio of the 10-year moving average CLM MNF divided by the stationary mean (average from 1954 to 1977); (c) the residual of CLM MNF with respect to its 10-year moving average MNF; and (d) the biased corrected runoff (RUN in Figure 9) constructed using Equation 6.

3. WATER SYSTEM MANAGEMENT

As shown in Figure 1, components of the IGSM provide inputs to a sub-model of water management, termed the Water Management System (WMS). Its structure is based on the Water Simulation Module of IFPRI's IMPACT-WATER model (Rosengrant, 2008). It computes the balance of water supply and water requirements⁶ for the network of 282 ASRs, treating each as a single water balance area with no sub-ASR geographic representation of the water resource system. **Figure 9** is a schematic of the WMS at the ASR scale. It provides a map of the way water flows in the process of balancing water supply with water requirements in the presence of within-year and over-year storage. All reservoirs in the ASR are aggregated into a single virtual reservoir, STO, in the figure.⁷ It is from this virtual reservoir that all surface water releases are made. The maximum storage STC is the sum of all the maximum capacities of the reservoirs in the ASR. This section provides an overview of the components of water flow in and out of this storage for each month and ASR and how they are linked within the WMS component of the overall model. To simplify the notation the indices for month and ASR are suppressed except where needed.

3.1 Water Supply

3.1.1 Surface Water Movements

Surface water enters the ASR storage from two sources. Runoff (RUN) is the natural flow from the ASR area defined in Section 2. Note that runoff as calculated may be diminished by surface water lost to groundwater recharge (GRW). RUN is then augmented by the flow into the ASR from one or more upstream ASRs (INF). The upstream-downstream links within the ASRs is established in the data set developed by IFPRI. Water then leaves the aggregated storage in three ways. Some is lost to evaporation (EVP); some is released to beneficial uses (REL), and some flows downstream to another ASR or to the sea (SPL).⁸

3.1.2 Groundwater

In this version of IGSM-WRS, groundwater is represented as a maximum monthly renewable (sustainable) supply, GRW, to meet water requirements. There is no modeled flow from groundwater to surface water. In future work, groundwater will be represented as a mass balance and elevation will be considered to better represent the effects of groundwater depletion. The current approach allows evaluation outside the model of the sustainability of the resource given

⁶ The term water "requirements" as used here does not convey the economic sense of a change in quantity demanded as a function of price and/or income but in the engineering sense of water needed to meet a specified target.

⁷ This representation leads to assessment issues in application to large basins with large spatial gradients in water supply and demands. This issue of scale is addressed in the WRS-USA model (Blanc *et al.*, 2012) and will be incorporated in later versions of the global IGSM-WRS.

⁸ Though not applied in applications shown here, provision can be made for water movement other than from upstream to downstream ASRs.

the projected use, and simulation of scenarios where maximum monthly renewable supply is adjusted to consider possible effects of depletion.

3.1.3 Desalination

One additional source of water supply is provided by desalination, (DSL) and is based on data on installed capacity.

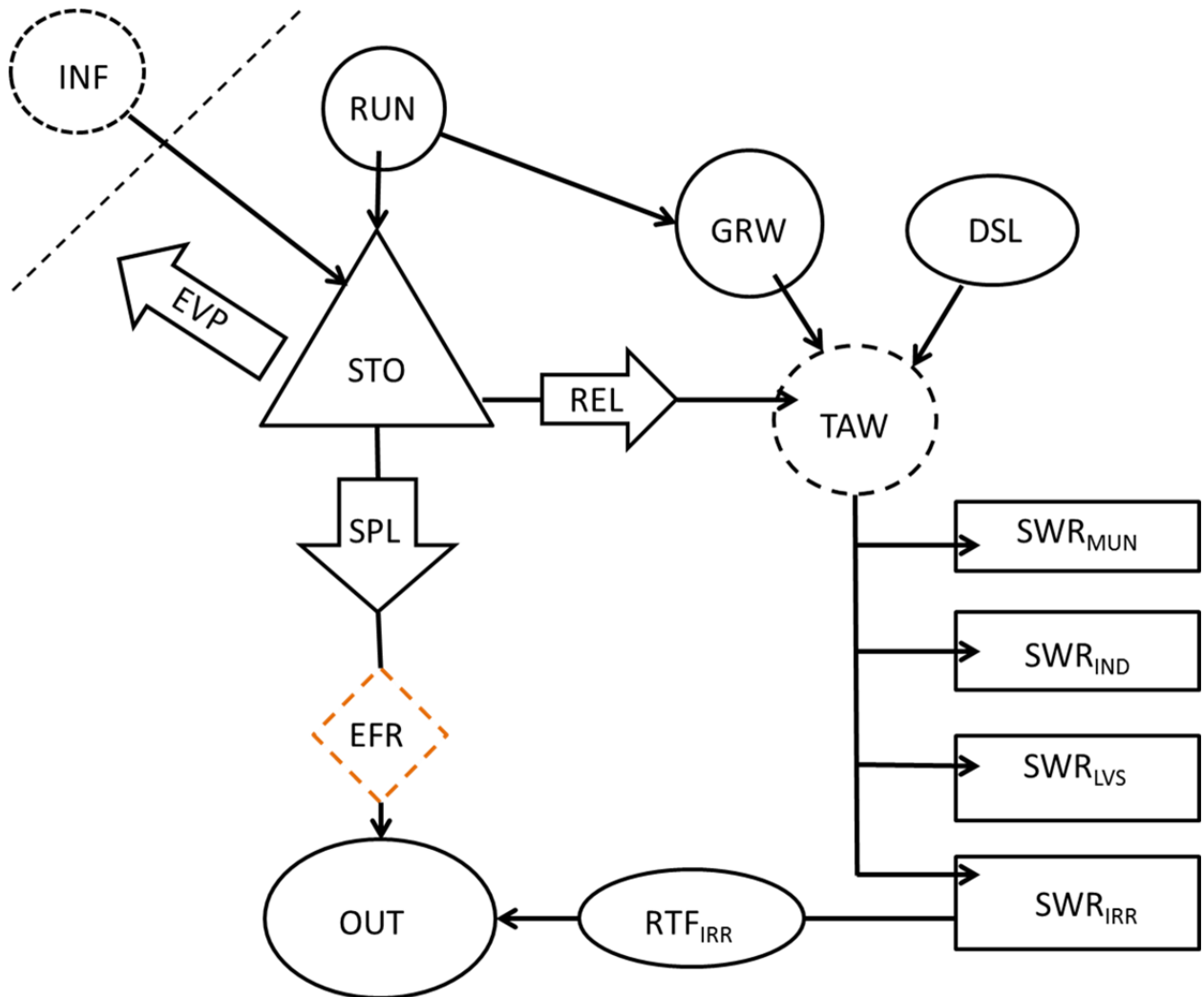


Figure 9. Water Management System operation at ASR scale in the IGSM-WRS. The total water requirement (TWR) is calculated by summing municipal (SWR_{MUN}), industrial (SWR_{IND}), livestock (SWR_{LVS}) and irrigation (SWR_{IRR}) requirements. Surface water supply comes from inflow from upstream basins (INF), and local basin natural runoff (RUN) and it goes into the virtual reservoir storage (STO) where evaporation loss (EVP) is deducted. The reservoir operating rules attempt to balance the water demands (TWR), with the total available water (TAW). Non-surface supplies: groundwater supply (GRW) and desalination supply (DSL), are used first and any remaining demands are met by a release from the virtual reservoir (REL). Additional releases (SPL) are made to meet environmental flow requirements (EFR).

3.1.4 Total Available Water

The WMS computes the total available water, TAW as the sum of surface water storage, groundwater supply and the desalination supply:

$$TAW = STO + GRW + DSL \quad (8)$$

where monthly STO is constrained by the surface storage capacity, STC.

3.2 Water Requirements

Water withdrawal is the total amount of water taken from the ASR water supply (storage, river, or aquifer) to provide for the various sectoral water uses, which then equals the total of consumption plus return flow (RTF). The following four sectoral water requirements (SWR in Figure 9) are modeled in the WRS, and their estimation is discussed in Sections 4 and 5.

Table 1. Water requirement sectors.

Sector	Abbreviation	Description
Municipal	MUN	Domestic, commercial and public uses
Industrial	IND	Agro-Industries, manufacturing and Energy
Livestock	LVS	On-Farm and stockyard
Irrigation	IRR	Crop consumptive use, conveyance and on-farm losses

3.2.1 Irrigation

The representation of ASRs as a single virtual storage renders the concept of classic irrigation system efficiency invalid because of the effects of recycling and a sequence of use cycles.⁹ To overcome the inconsistencies associated with classical efficiencies, the concept of effective efficiency was developed by Keller and Keller (1995) and advanced by the International Water Management Institute for use in water resource planning (Keller *et al.*, 1995). Irrigation system efficiency (*SEF*) is defined as the ratio of crop consumptive use over the entire ASR to the total amount of water delivered to irrigated lands. In the WMS formulation, return flow from irrigation is downstream of the virtual reservoir so is not available for other uses, and therefore the sector water requirement for irrigation is defined as:

$$SWR_{IRR} = WTH_{IRR} = \frac{CON_{IRR}}{SEF} \quad (9)$$

where CON_{IRR} is the water consumption in irrigation, computed in Section 4.1 below. The return flow from irrigation then is:

$$RTF_{IRR} = WTH_{IRR} - CON_{IRR} \quad (10)$$

⁹ Egypt's Nile irrigation system is an excellent example of a multiple use-cycle system with a high global efficiency but low local efficiencies. Keller and Keller (1995) estimate for the Nile-Egypt ASR that the classical irrigation efficiency for the major irrigation system to be 41.2% while the effective irrigation efficiency for the ASR to be 91.3%.

3.2.2 Non-Irrigation

Municipal, industrial and livestock requirements are assumed to be independent of climate, while irrigation requirements are driven by monthly temperature and precipitation. The non-irrigation water uses (municipal, industrial and livestock) consume only a small portion of the water withdrawal requirement. Also, the global average ratios of consumption to withdrawal for municipal, industrial and livestock are approximately 10%, 12% and 10% respectively (UNEP, 2008), with the remainder returned for use by other water users nearby. Because this return flow is near to the point of withdrawal (which is not the case for irrigation) it can be assumed that the return flow is to the virtual storage, and so the sectoral water requirement, SWR , for each of the four above is estimated as its water consumption.

3.2.3 Total Water Requirement

Each month WMS determines the amount of water to be released from the virtual reservoir (REL) to be combined with the supply from groundwater and desalination to yield the Total Available Water (TAW) where:

$$TWR = SWR_{MUN} + SWR_{IND} + SWR_{LVS} + SWR_{IRR} \quad (11)$$

3.2.4 Environmental Flow Requirement

Each month WMS must release water from the virtual reservoir to provide minimum flows (EFR) for the maintenance of aquatic ecosystem services including floodplain maintenance, fish migration, cycling of organic matter, maintenance of water quality or other ecological services (Smakhtin, 2008). IFPRI has established minimum monthly and annual outflows from the 282 ASRs stated as a percentage of mean annual runoff. In some cases these flow requirements are currently not being met due to extensive irrigation consumption. For the base case in 2000 these constraints have been adjusted to reflect current conditions.

3.3 Supply-Demand Balance

Each month the algorithm first balances water supply and demand in each ASR, beginning at the most upstream ASR and working downstream. If there is insufficient supply to meet all requirements in an ASR it then allocates the available water among its sectors.

3.3.1 The ASR Water Balance and Virtual Reservoir Operation

The model is formulated as a mathematical programming problem, solved simultaneously for the 12 months of each year, y . The model objective is to keep as much water as possible in storage and maintain the minimum environmental flow while providing a total water supply, TWS , that satisfies as much as possible of the four sectoral water requirements. The algorithm used here is one of several developed by IFPRI (Rosengrant, 2008), with four components.¹⁰

¹⁰ Alternative formulations are under study at both MIT and IFPRI.

First, a variable, RA , is defined to capture the performance of the model in meeting the water requirement in each month:

$$RA(m) = \frac{TWS(m)}{TWR(m)} \quad (12)$$

where $TWS(m)$ is the water actually supplied and $RA < 1.0$ indicates shortage. Within this part of the objective, however, there is a desire not to penalize any particular month, so a minimum level of monthly shortage, MRA , also is included:

$$MRA(y) = \min_y [RA(m)] \quad (13)$$

Then, to manage the available storage two variables are added, one to meet as much of the requirement as possible from runoff instead of groundwater, and one to limit unnecessary spillage. Following the IFPRI procedure a simple sum of these components leads to the following expression:

$$\max \left[\sum_{m \in y} RA(m) + MRA(y) + \frac{TWS}{RUN} - \frac{SPL}{RUN} \right] \quad (14)$$

subject to the storage accounting and limits on its capacity and a minimum level:

$$\begin{aligned} STO(m) &= STO(m-1) + RUN(m) + INF(m) + DSL(m) - GRC(m) - REL(m) - SPL(m) - EVP(m) \\ STO(m) &\leq STC(m) \\ STO(m) &\geq STC(m) * 0.1 \end{aligned} \quad (15)$$

It includes the calculation of supply from the virtual storage and groundwater and imposition of the environmental flow requirement:

$$\begin{aligned} TWS(m) &= REL(m) + GRS(m) \quad \text{and} \\ SPL(m) &\geq EFR(m) \end{aligned} \quad (16)$$

Finally, there is the calculation of evaporation based on the average storage in the month, where NET is the net evaporation (evaporation minus precipitation) over the surface storage area:

$$EVP(m) = NET(m) \frac{(STO(m) + STO(m-1)) / 2}{STC(m)} \quad (17)$$

3.3.2 Water Allocation

The model allocates available water among sectors following simple priority rules, reflecting differences in the value of water in different uses. If the total water available is insufficient to meet total water requirements, water is first allocated equally among the municipal and industrial sectors, with each given the same fraction of the amount supplied. Irrigation and livestock sectors are last in priority and are served only if there is sufficient water to meet all industrial and municipal requirements. The algorithm can be easily changed to reflect institutional

arrangements, such as legally established water rights, that may lead to a different rule in any particular ASR.

4. AGRICULTURAL WATER USE

4.1 Irrigation Water Requirement

4.1.1 Potential Evaporation

Runoff is the difference between precipitation and *actual* evapotranspiration, which is directly related to potential evapotranspiration (PET). In this application net irrigation water demand is calculated as crop water demand minus precipitation, and PET is an input into the calculation of the demand by different crops (Fant *et al.*, 2012). PET is therefore, a crucial variable relating climate conditions and water supplies and requirements. The IGSM-WRS employs the Modified Hargraves Method for estimating reference crop PET, here denoted MH-PET (Farmer *et al.*, 2010). **Figure 10a** is a map of mean annual MH-PET calculated from IGSM downscaled climate data at 2.0° latitude by 2.5° longitude, averaged over the period 1970 to 1990. **Figure 10b** is a map of mean annual MH-PET calculated from observed climate data at a 0.5° by 0.5° averaged over the period 1970 to 1990 (CGIAR, 2012). The maps show a strong correspondence at broad scale of regions of high and low MH-PET.

Figure 11 is a plot of the mean annual MH-PET from the downscaled IGSM climate versus the CGIAR values spatially averaged over the 282 ASRs. The results show good agreement except for a string of outliers that have much higher values when calculated based on observations. These outliers are island nations or very small nations on the coast where the IGSM downscaled grid cell is larger than the ASR land area. The inclusion of cooler ocean temperatures into the PET calculation leads to an underestimate of PET.

To further investigate PET estimation in the IGSM-WRS we compare the monthly MH-PET with results from a temperature-only method, Blaney Criddle (BC-PET). Better data availability allows this comparison to be done for a 99 ASR aggregation of the U.S. The comparison is made for two observational data sets (CRU at 0.5° by 0.5° and PRISM at 2.5-arcmin [4 km] grid) and the IGSM-WRS simulated climate. **Figures 12a-c** shows results for three sample basins: the North and South Platte, the Upper Central Snake and the San Joaquin-Tulare.

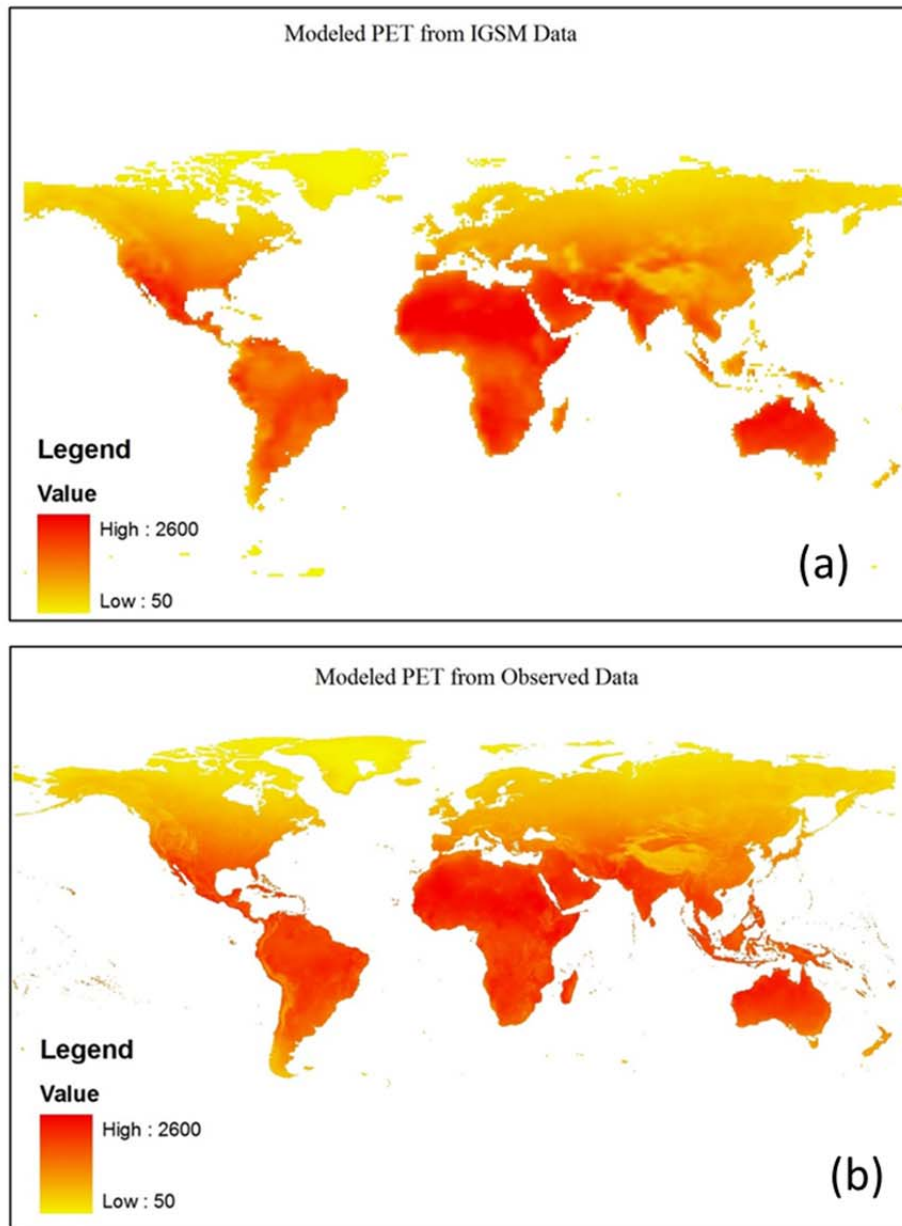


Figure 10. Global maps of mean annual potential evapotranspiration (PET) modeled with the Modified-Hargreaves method and averaged over 1970 to 1990 using, (a) the IGSM downscaled precipitation and temperature, and (b) as estimated by CGIAR (2012) using CRU observed precipitation and temperature (New *et al.*, 2005).

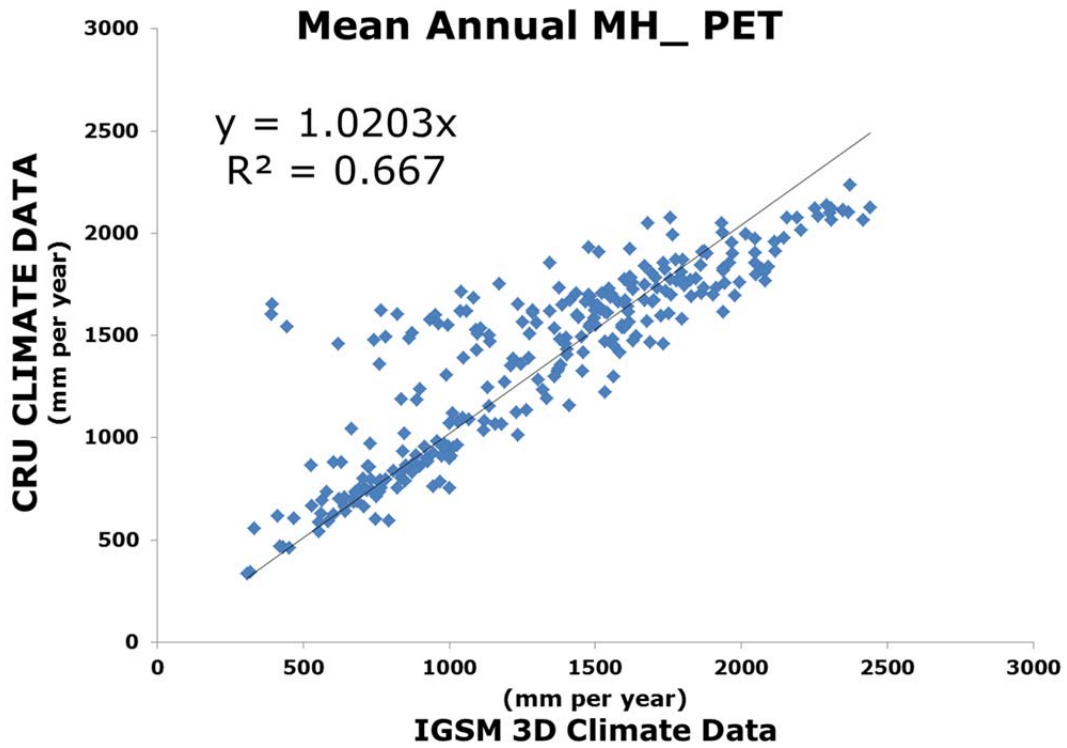


Figure 11. Comparison of mean annual potential evapotranspiration (PET) modeled with the Modified-Hargreaves method and averaged over 1970 to 1990 between the IGSM downscaled precipitation and temperature (x-axis) and the CRU observed precipitation and temperature (y-axis) for the 282 global Assessment Sub-Regions of the IGSM-WRS.

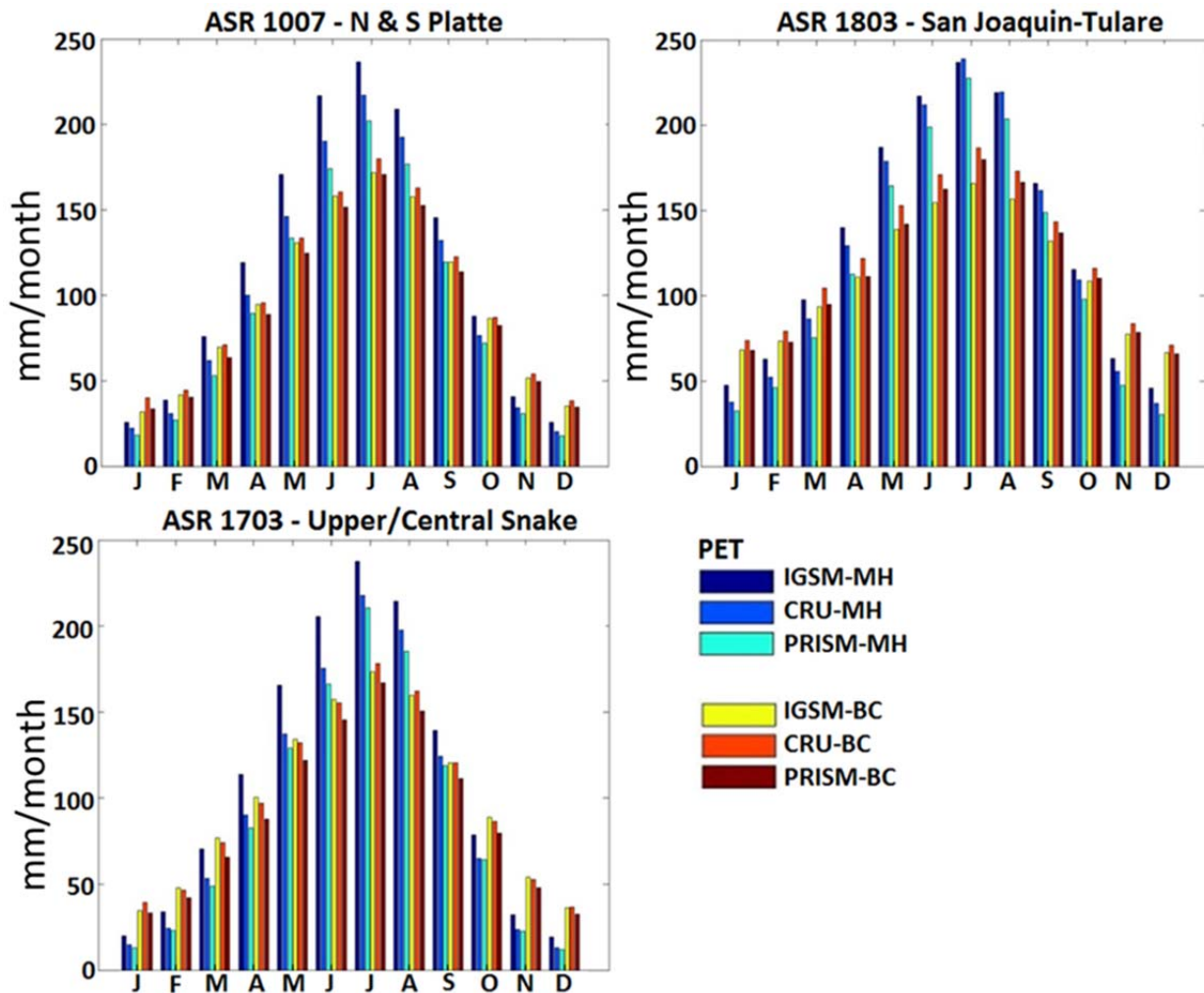


Figure 12. Estimates of monthly potential evapotranspiration (PET) using the Modified Hargreaves (MH) method, an approach that utilizes both temperature and precipitation, and the Blaney-Cridde (BC) method based only on temperature. Using MH and BC algorithms three climate data sets are compared. CRU and PRISM are observation based, and one is based on downscaled IGSM data. Results are averaged over the period 1961–1990 and shown for three U.S. basins: North and South Platte, San Joaquin-Tulare and Upper and Central Snake.

Several points are worth noting in these results. First, there are differences in the PET estimate between the two observation-based data sets for both MH-PET and BC-PET procedures. Second, the differences across data sets are greater for MH-PET than for BC-PET. This is attributable to the fact that MH-PET uses both precipitation and temperature whereas BC-PET considers temperature alone, so the MH procedure adds a variable that is more uncertain across space. Finally, the IGSM-WRS procedure performs well seasonally for these basins and is within the variability introduced by the different observation data sets. We judge the fit to be satisfactory for use in the agricultural sub-model.

4.1.2 Water Consumption at the Root

Crop consumptive use is the main element of the irrigation system related to climate. Here we describe a formulation, used at the 282 ASR or global level, where the crop is given water at the root for maximum yield. This quantity is estimated using CliCrop, a generic biophysical crop model developed for integrated assessment frameworks. It is global, numerically efficient and as used in WRS makes use of the limited set of inputs available globally (Fant *et al.*, 2011). CliCrop is based on FAO's CropWat model (Allen *et al.*, 1998) for the crop phenology and irrigation requirement, and on the SWAT model (Neitsch *et al.*, 2005) for the soil hydrology. CliCrop runs on a daily timescale and has a 2° by 2.5° grid resolution for the globe. It estimates crop water requirement (in mm/crop/month) to obtain maximum yield under simulated weather conditions. The irrigation demand at the roots of the plant is defined as the difference between the evapotranspiration demand (as defined by Allen *et al.*, 1998) and precipitation. CliCrop determines irrigation requirements for 13 of the most commonly grown crops.

To estimate irrigation requirements for crops modeled in WRS but not modeled by CliCrop, proxy crops with similar crop irrigation needs were chosen. For each crop modeled with CliCrop, the planting date has been specified according to available data from SAGE – University of Wisconsin (Sacks *et al.*, 2010).

Monthly crop consumptive requirements for each ASR are provided to the WRS. CliCrop provides an estimate of the monthly crop consumptive use per unit of land (hectare) as irrigation depth in mm, $IRR_{mm}(crop)$. The area of each crop $IRR_{area}(crop)$ is an input to WRS and the crop consumptive use is then:

$$CON_{IRR} = \sum_{crops} (IRR_{mm} * IRR_{crop}) \quad (18)$$

4.1.3 Delivery Efficiencies

To estimate the water needed to supply consumption at the root the hierarchical nature of irrigation systems needs to be considered. Water withdrawn at the source (e.g., stream, reservoir) is delivered to the field via a conveyance system (e.g., canals and pipes). Water withdrawn that is lost through seepage and/or evaporation on the way to the field is known as conveyance loss. One minus the fraction of water lost is termed the conveyance efficiency. For unlined canals the efficiencies ranges from 60% to 90% depending on the soil type. Length and poor canal maintenance can greatly reduce conveyance efficiency. Not all the water delivered to the field is useful to the crop, and field efficiency depends on the type of irrigation system used (e.g., sprinkler, drips). Furthermore, crop value and other considerations may lead to management decisions at the farm where an amount of water different than that needed for maximum yield is applied. In applications where the data permit (e.g., in the U.S., see Blanc *et al.*, 2012) these factors are taken into account as they differ by region and crop. However, at the 282 ASR global level the IGSM-WRS does not distinguish conveyance and field efficiencies and management factors, but instead represents irrigation as a single system efficiency to compute SWR_{IRR} as applied in Equation 8.

4.2 Livestock Water Use

Livestock water consumption SWR_{LVS} is estimated based on livestock numbers and water consumptive use per unit of livestock, which includes beef cattle, cows, pig, poultry, eggs, sheep and goats, and aquaculture fish production. Its projection of numbers is assumed to be proportional to demand in the agricultural sector in the EPPA model with no change in consumptive water use per head.

5. NON-AGRICULTURAL WATER USES

For the current version of the IGSM-WRS applied at global scale, base-level non-agricultural water requirements are based on estimates in the IFPRI's IMPACT model (Rosengrant *et al.*, 2008). These base-level requirements are projected to change as a function of projected population and economic growth, which for consistency with the climate projections we take from the EPPA model (see Figure 1). EPPA models the global economy in 16 regions, r , and the global configuration of the IGSM-WRS models non-agricultural water demand at 282 ASRs (see Figure 2). An assumption of homogeneity of growth for the IGSM-WRS economic regions within each EPPA region was used to downscale EPPA projections. The method produces annual water requirements, which are distributed evenly across months. In this version of the IGSM-WRS system we focus on representing water supplies and requirements, and allocating available supplies among uses at a basin scale under varying scenarios of future climate, energy policy and economic growth. The addition of feedbacks of changes in water availability on the economy and energy supply is scope for future research.

5.1 Municipal Water Use

Municipal requirements include domestic use (urban and rural), public use, and commercial use connected to a municipal water system. The method is based on projections of growth rates of population and per-capita income, ϕ_{POP} and ϕ_{PCI} for each EPPA region. Income elasticities of demand for municipal water to GDP (η) also are estimated for each economic region, n (see Appendix). The annual growth rate of municipal water requirement for each economic region in each year y , $\phi_{MUN}(n)$ is then:

$$\phi_{MUN}(r) = \phi_{POP}(r) + \eta(r) * \phi_{PCI}(r) \quad (19)$$

for all economic regions n in EPPA region r .

If $\eta < 0$ and income growth is greater than population growth, municipal water requirements will decline, which has been observed in some developed countries. Where $\eta > 0$ municipal water requirements will increase.

These growth rates are applied to each ASR within an economic region, weighted by population, so that for each ASR the water requirement becomes:

$$SWR_{MUN}(y) = SWR_{MUN}(y-1) * (1 + \phi_{MUN}) \quad (20)$$

where SWR_{MUN} for the 2000 base year for each ASR has been estimated from FAO AQUASTAT data and information on the population distribution within countries.

5.2 Industrial Water Use

The model identifies three industrial water use sectors: manufacturing and service, energy production and thermal electric cooling, and agro-industrial. Changes in requirements for each industrial water use sector are based on estimates of the elasticity of water use to per-capita GDP, η_{GDPC} , with adjustments for time and the particular nation. For each of the three sub-sectors, where α_n is the economic region intercept. This estimate is then augmented by parameter:

$$\log(SWR_{IND}) = \alpha_n + \eta_{GDPC}(n) \log[GDPC(r)] + \gamma_n * y * ADJ_n \quad (21)$$

for growth over time, γ_n , adjusted by factor, ADJ_n to account for countries where growth in GPDC does not properly capture structural changes or reflect climatic or water availability factors. The general pattern observed is that water industrial water requirements grow as a nation industrializes and then slows or even declines at higher levels of development with changing structure of industry and policies that lead to greater water reuse, recycling.

The estimates of $SWR_{IND}(n)$ for each industrial sub-sector are then allocated among the ASRs within a nation according to the geographical distribution of industry, using population as a surrogate.

6. ASSESSMENT OF MODEL PERFORMANCE

A challenge for global water model development is the lack of data against which the model performance can be evaluated. Many key variables are estimated using models or where data exists it is often considered to be of poor or varying quality or available for a very limited period. Here we assess the performance of the model in comparison with historical data where available, and in other cases we compare against other modeling exercises.

The first step in this assessment is to calibrate the model over an initial historical period and then to simulate a second historical period that was not used in the model calibration. **Figure 13** shows the IGSM-CLM runoff (Q_{CLM}) for these two periods and the 10-year moving average of IGSM-CLM runoff (Q_{CLM}) $\mu_{CLM_MA10}(m,y)$. The ratio of the 10-year moving average of Q_{CLM} after 1977 over the stationary mean of Q_{CLM} over the period 1954 to 1977, $\mu(m)_{CLM}$, becomes the normalized trend of Q_{CLM} ($TrCLM$) described in Equation 5. As previously noted, the MOVE calibration of CLM is based on the period 1954–1977. Then the model is evaluated for the period 1980–2000, driven by the simulated climate. Model results are then compared with observations or observation-driven constructions of the water system performance.

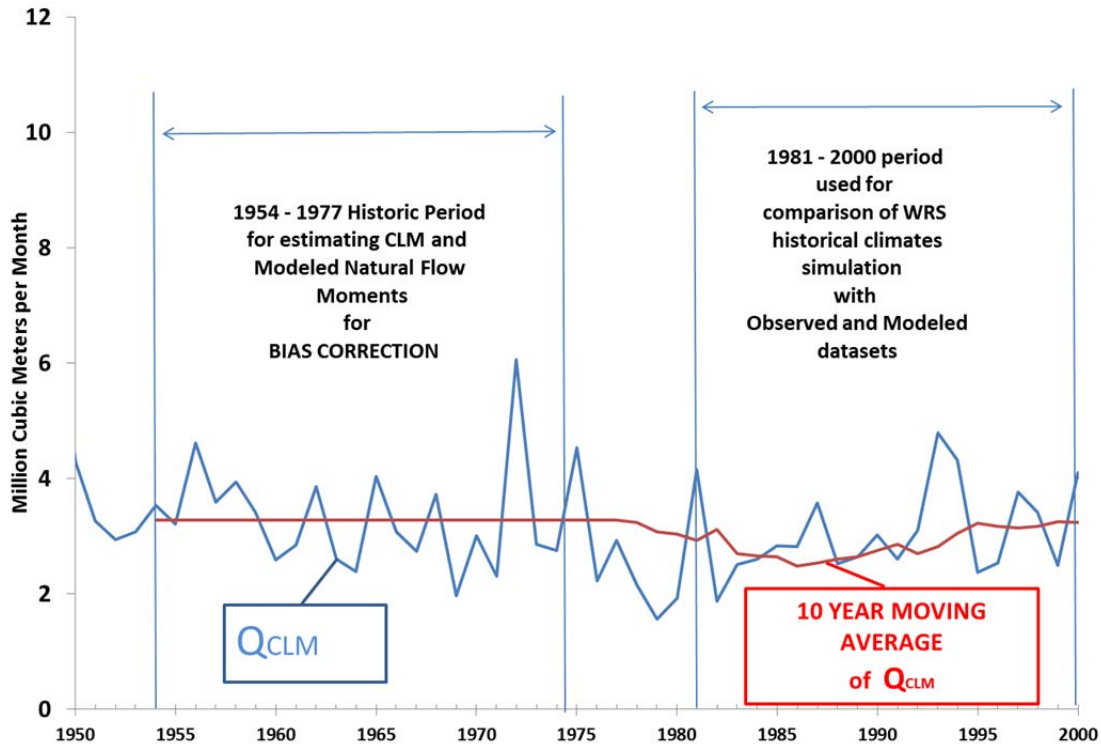


Figure 13. Timeline of calibration and comparison windows for IGSM-WRS (Q_{CLM}) and observed runoff data. For 1954 to 1977 climate is considered stationary with constant means and variance, and the period is used to calibrate model components and develop bias-correction parameters. After 1977, the climate is assumed to be non-stationary with runoff means having a trend from a changing climate, defined by a 10-year moving average (mean Q_{CLM}) while variances remain constant. IGSM-WRS simulations are then compared with observed and modeled historical data over the period 1981 to 2000.

6.1 Results at the Global Scale

Results are mapped for IGSM-WRS simulated variables averaged over the assessment period 1981–2000 for the 282 ASRs, and scatter plots with regression estimates are also presented to compare IGSM-WRS simulations with observations.

6.1.1 Runoff

Figure 14a shows that IGSM-WRS runoff exhibit the expected spatial variability and arid and humid conditions are found where expected. **Figure 14b** provides a visual confirmation that IGSM-WRS is representative of historic conditions over 1981 to 2000 as estimated by IFPRI-MNF (Zhu *et al.*, 2012). The mean global runoff for IGSM-WRS and IFPRI-MNF averaged over 1981 to 2000 are 39,950 and 40,260 billion cubic meters, respectively. These values are further apart than over the 1954–1977 calibration period. **Figure 14c** is a scatterplot of the spatial correlation of the mean annual runoff of the IGSM-WRS runoff versus the IFPRI-MNF for the 282 ASRs for the assessment period 1981 to 2000. The slope of the linear regression line through

the origin of 1.0252 suggests that geographical climate signals driving both series are similar between the calibration and assessment periods. As expected the IGSM-WRS and the IFPRI-MNF are not as similar as over the calibration periods. This vetting of the bias-correction method over the assessment period provides more validation to effectiveness of the non-stationary MOVE extension.

6.1.2 Irrigation Requirements by Crop

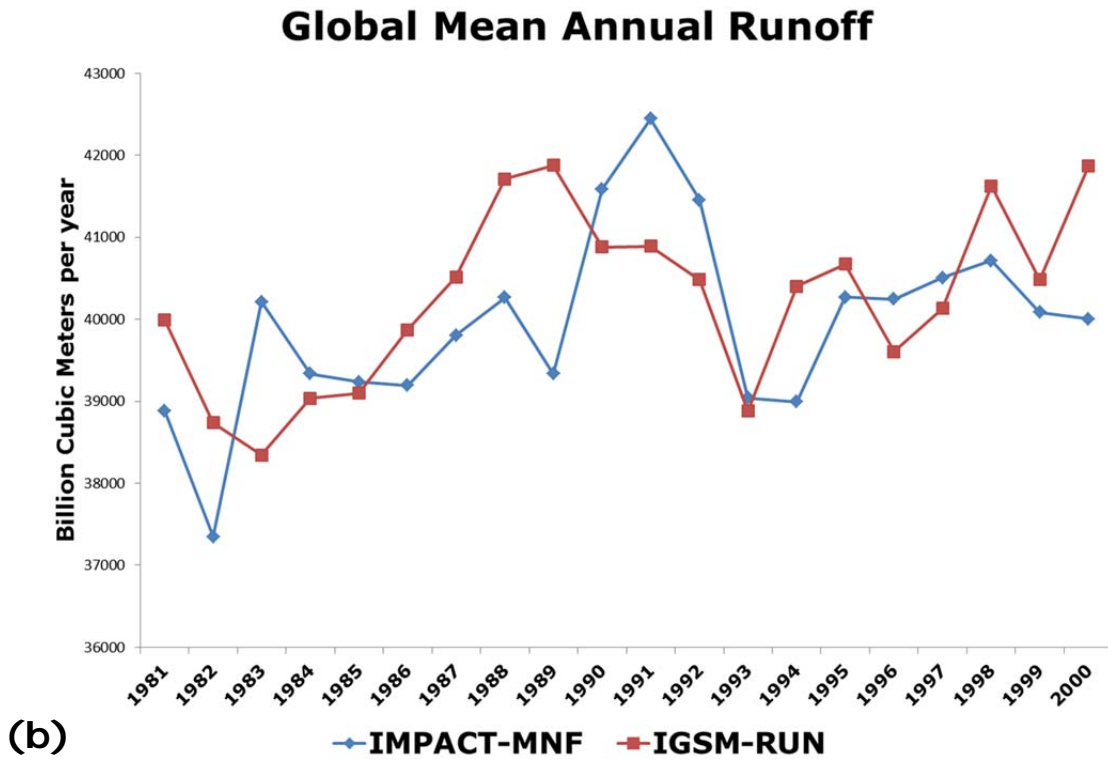
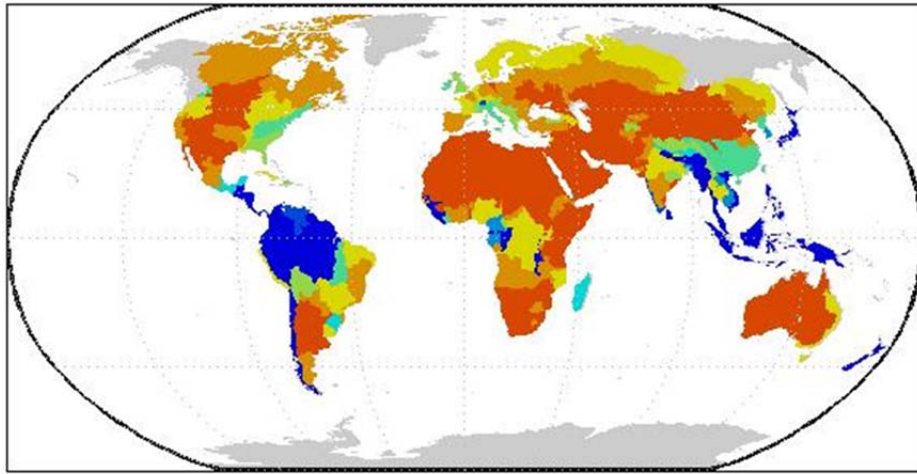
Figure 15a shows IGSM-WRS annual irrigation demand for maize from CliCrop. It exhibits the expected larger values in arid regions and lower values in humid regions. (Though essentially no maize is grown in the extremely water short regions such as the Sahara Desert and the Arabian Peninsula, CliCrop calculates for those ASRs as well, naturally showing the maximum irrigation demand in the figure.) **Figure 15b** provides confirmation that in the IGSM-WRS CliCrop maize irrigation requirement is roughly consistent ($R^2=0.61$) with estimates for the IIASAs-FAO GAEZ model (Fischer, 2012), which is representative of historic conditions. The results show similar agreement for all other crops modeled in the IGSM-WRS.

6.1.3 Water Requirements by Sector

Global databases on water use are a recent phenomenon so historical time series data are lacking. The FAO has developed a comprehensive online database of water use, AQUASTAT (FAO, 2012). The data are presented at a country level, requiring IGSM-WRS results to be aggregated to the economic region level. Also, AQUASTAT has limited temporal data, but its estimates for 2000 provide a basis for comparison. A comparison exercise was undertaken by running IGSM-WRS for the period 1981 to 2000 with irrigation areas and non-agricultural demands held constant at year 2000 base-levels. The annual output of IGSM-WRS were averaged over the period and compared to FAO data on water requirements for 2000. The global climate over 1981 to 2000 is representative of the drivers in FAO 2000 data. A measure of IGSM-WRS's ability to adequately model the global systems would be the similarity of average 1981 to 2000 IGSM WRS outputs and the FAO reported data. Figures 16–18 show the IGSM-WRS simulation averages from 1981 to 2000 versus AQUASTAT data for the year 2000.

Figure 16 shows total irrigation demand. The comparison shows close correspondence (R^2 of 0.81) with the exception of three outliers where the WRS estimate is below that in AQUASTAT. The two extreme outliers are for Indonesia and Japan, both island nations where the scale of the IGSM grids leads to lower irrigation demand due to differences in land and ocean temperature and precipitation. The less extreme outlier is Iran where data on irrigated areas used in IGSM and the data reported in FAO has a high degree of uncertainty.

Figure 17 is the same comparison for municipal requirements. This fit also is very close (R^2 of 0.81) with the exception of two outliers. There are a few outliers where the IGSM-WRS over-predicts water and has a slight bias toward over-prediction of use compared to AQUASTAT.



Mean Annual Runoff 1981-2000

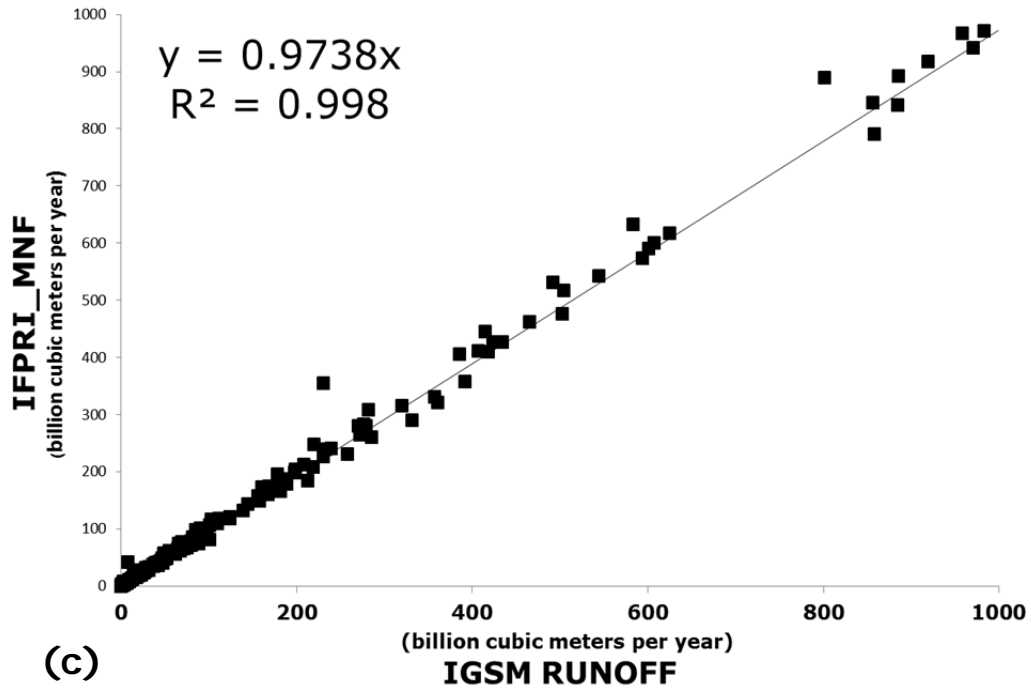
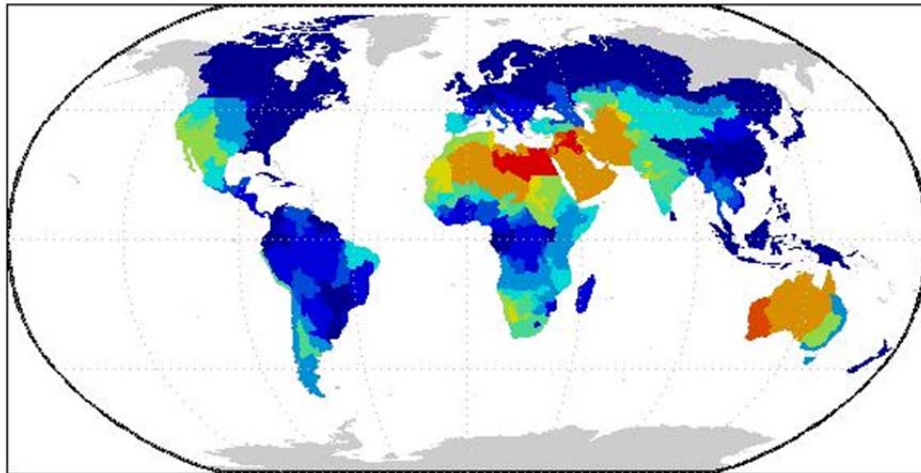


Figure 14. IGSM-WRS mean annual natural runoff for the period 1981 to 2000 presented as: (a) a map of the 282 ASR annual runoff and; (b) annual global runoff time series of IGSM-WRS and IFPR-MNF for 1981 to 2000; and (c) a scatterplot comparing IFPRI mean annual Modeled Natural Flow (MNF) in billions of m³ per year with the WRS estimate for 282 ASRs. Statistics are for a linear regression of IFPRI MNF on WRS estimated values.



(a) **Annual Irrigation Requirement for Maize Under WRS Global (mm)**

< 100 200 300 400 500 600 700 800 900 1000 >

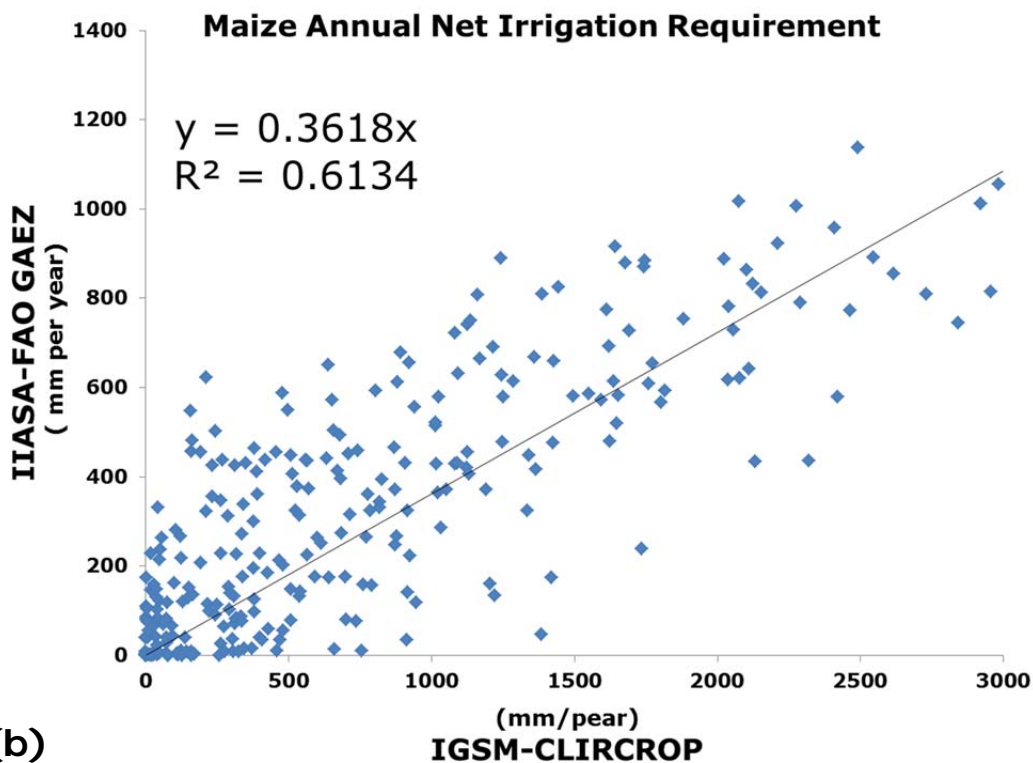
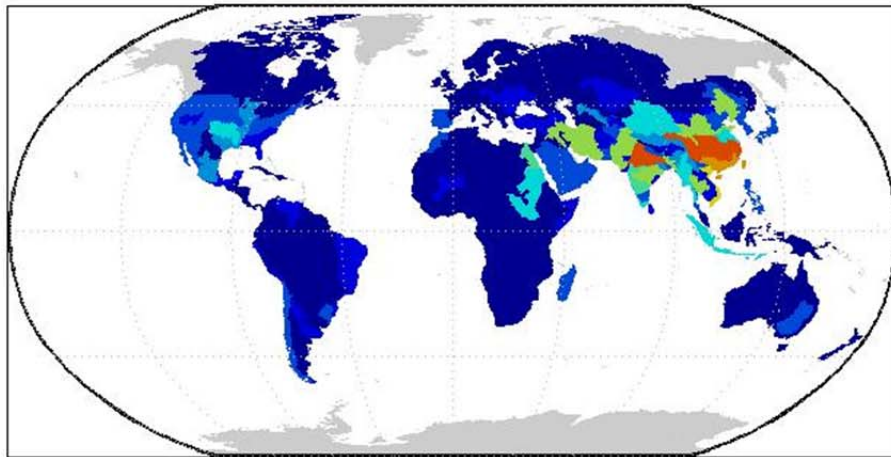
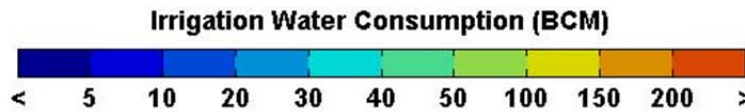


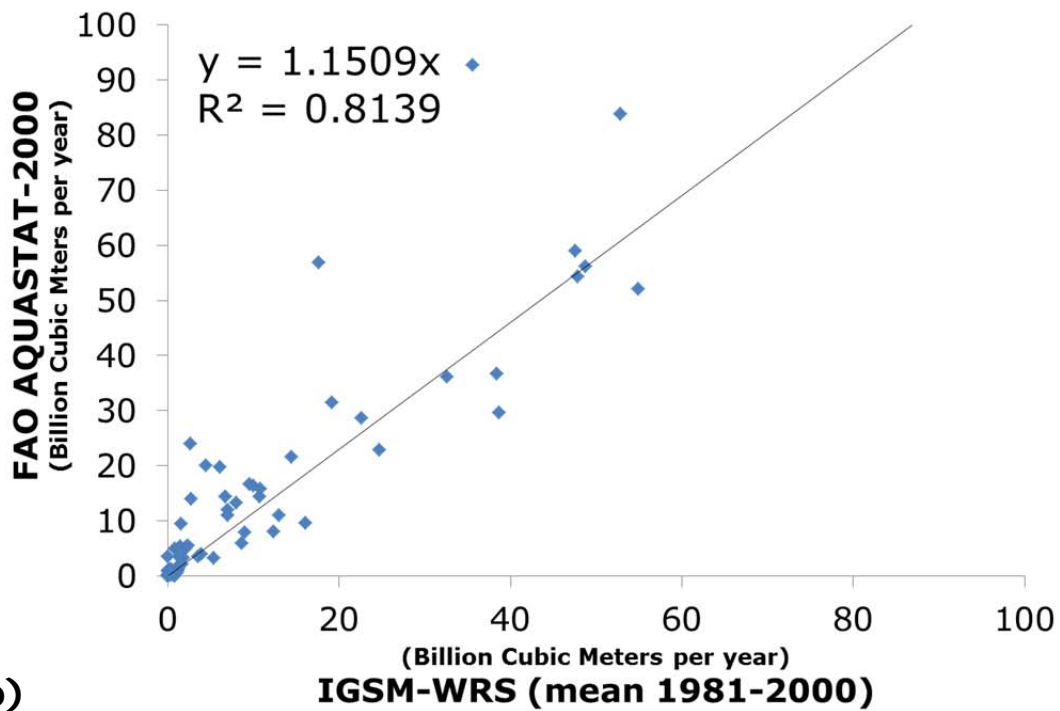
Figure 15. Results for IGSM-WRS maize irrigation requirements averaged for the period 1981 to 2000 presented as: (a) a map of the 282 ASR values; and (b) a scatterplot comparison of 1981–2000 mean maize irrigation demand between the IIASA-FAO Global Agro-Ecological Zone crop model and the WRS-CliCrop crop model for the 282 ASRs. Statistics are for a linear regression of IIASA FAO on WRS estimated values.



(a)

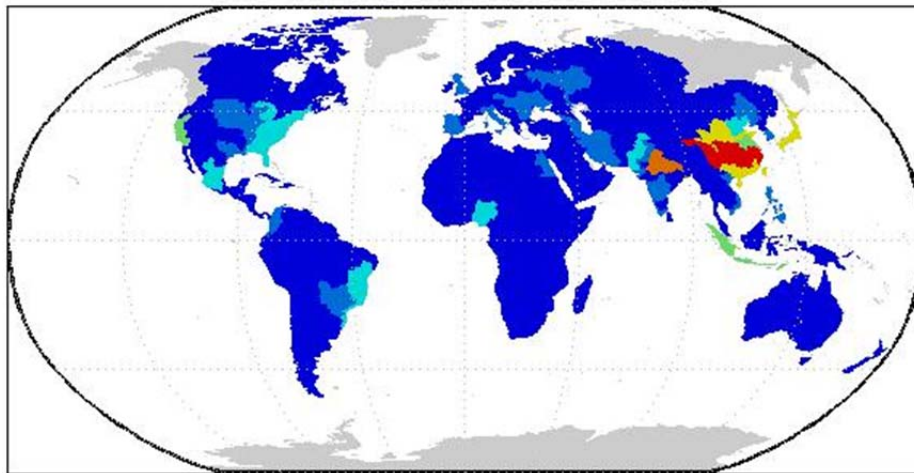


Annual Irrigation Requirement



(b)

Figure 16. IGSM-WRS total irrigation demand averaged for the period 1981 to 2000 presented as: (a) a map of the 282 ASR annual values (in billions of m³); and (b) a scatterplot comparison between WRS-CliCrop estimates and FAO AQUASTAT data by countries. Statistics are for a linear regression of AQUASTAT data on WRS estimated values.



(a)

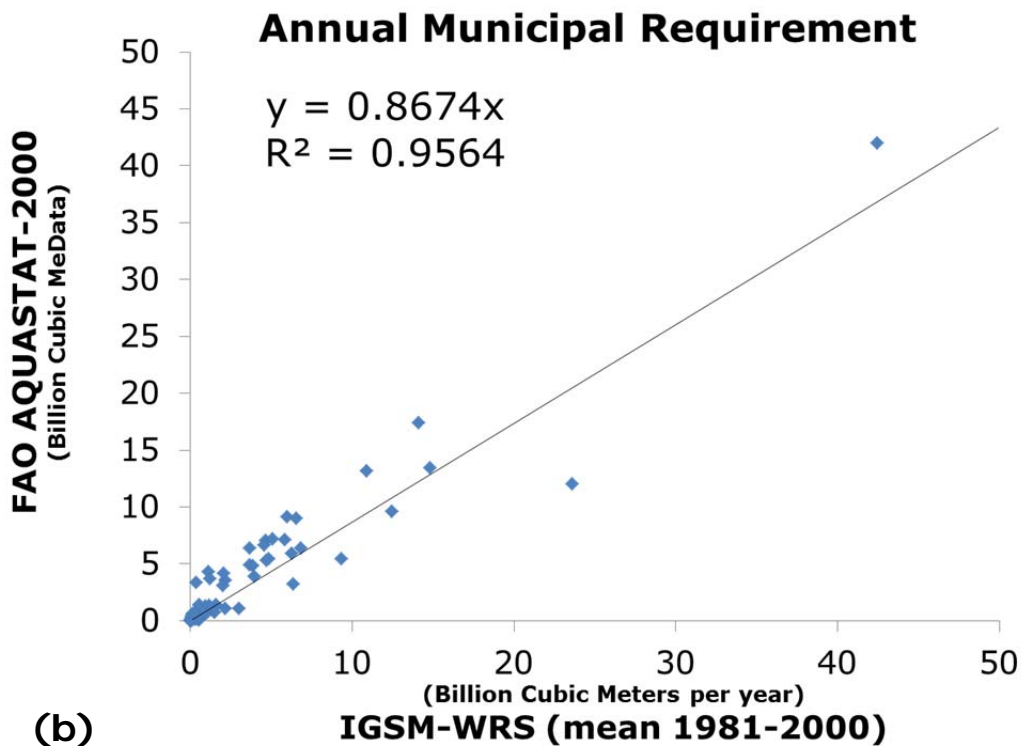
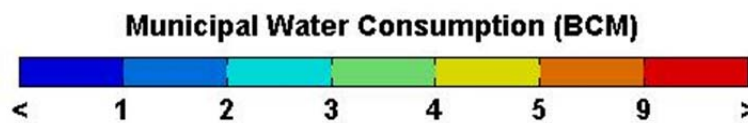
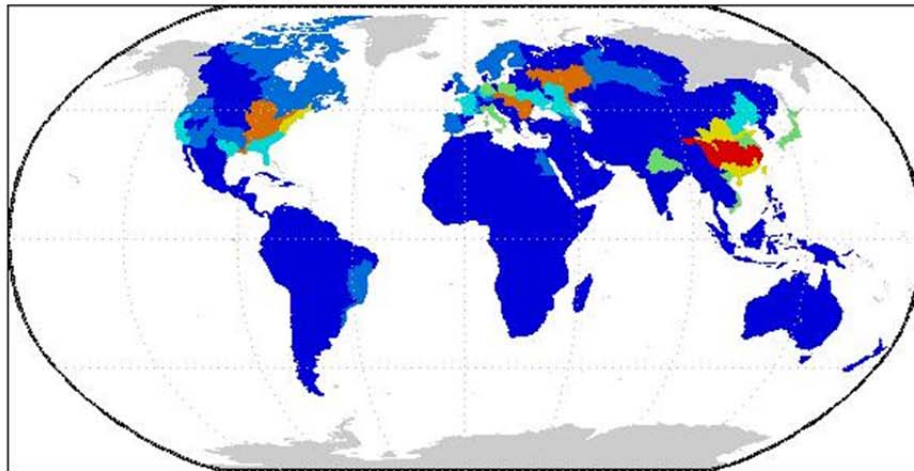
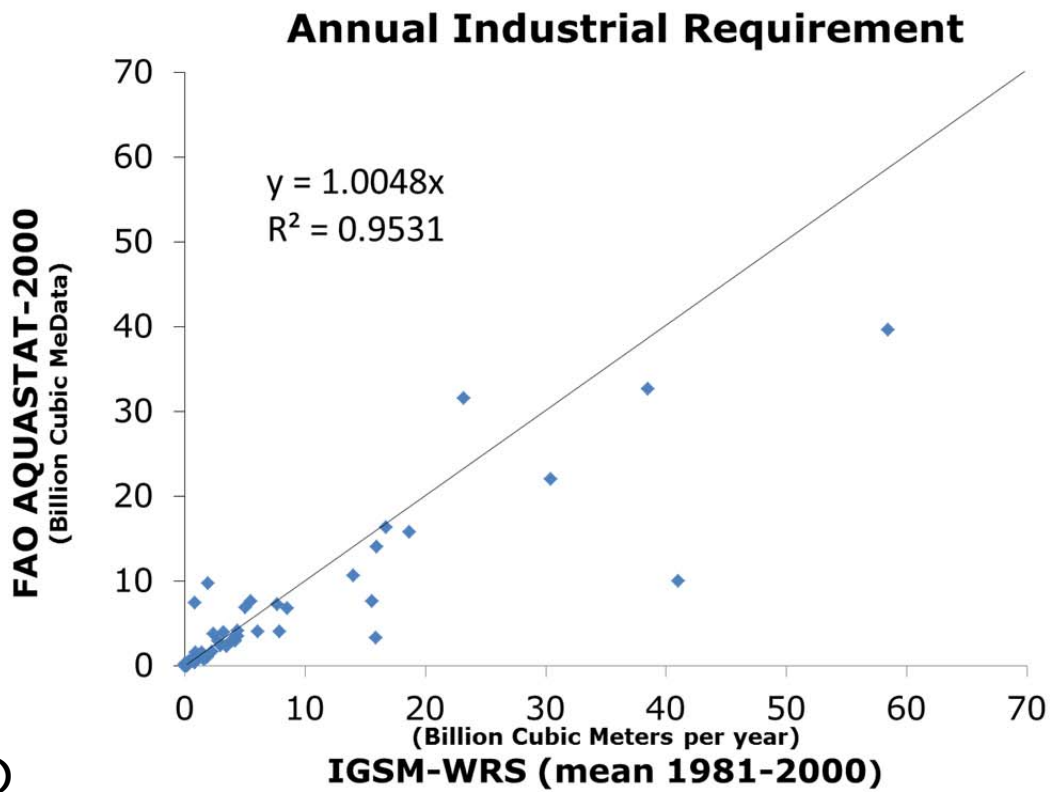
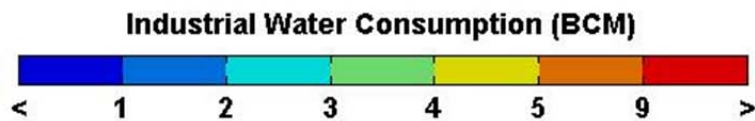


Figure 17. IGSM-WRS total municipal water requirement averaged for the period 1981 to 2000 presented as: (a) a map of the 282 ASR values (in billions of m³); and (b) a scatterplot comparison between IGSM-WRS estimates and FAO AQUASTAT data (by country). Statistics are for a linear regression of AQUASTAT data on WRS estimated values



(a)



(b)

Figure 18. IGSM-WRS total industrial withdrawal averaged for the period 1981 to 2000 presented as: (a) a map of the 282 ASR annual values (in billions of m³); and (b) scatterplot comparison of between IGSM-WRS estimates and FAO AQUASTAT data by country. Statistics are for a linear regression of AQUASTAT data on WRS estimated values.

Figure 18 is the IGSM estimate of industrial requirements, and here the correspondence with the AQUASTAT data is extremely close (R^2 of 0.95). The outliers where the IGSM-WRS overestimates industrial withdrawal are India and Russia. This is the result of using a single global industrial withdrawal to consumption ratio, which varies depending on the structure of the economy.

6.2 Results at the Basin Scale

Figures 16–18 show results at the level of economic regions, but because most of these contain several ASRs the results can hide compensating errors. Also, the results sum over a considerable time period. Because beneficial use of water and the impact of water management are felt year-to-year at the local or basin level, the usefulness of a model for impact assessment depends on its fidelity at this finer scale. Thus we explore model performance in greater detail by considering four ASRs that represent a range of conditions: large irrigation demand, large reservoir storage and large spatial area. Together these basins present a broad range of water management conditions for a modeling framework like the IGSM-WRS to accurately model:

- **The Nile Basin in Egypt:** No effective local runoff, large irrigation demand, large reservoir storage and downstream of a major transboundary river basin. Homogeneous irrigation needs;
- **The Nile Basin in Sudan:** large irrigation demand, large reservoir storage, major downstream transboundary flow requirements, large internal local runoff, Homogeneous irrigation needs;
- **The Murray-Darling River in Australia:** Large irrigation demand, large reservoir storage, no downstream requirements and not a transboundary river basin, homogeneous irrigation needs;
- **The Missouri Basin in the U.S.:** Large spatial area, non-homogeneous, hydro-climatically, across the basin, large reservoir storage, supplemental irrigation needs.

6.2.1 Runoff

As with the earlier comparisons we follow the procedure where the IGSM-WRS is calibrated to 1954 to 1977 and the period 1981 to 2000 is simulated for comparison with the IFPRI MNF values. The ASR level precipitation and temperature over the 20-year period is not expected to be identical yearly or monthly because the results are driven by climate model output with variability like that observed but not directly matching the observations for specific years. However, the model results, if reasonable, should show a similar long-term mean and general pattern of variability. The performance of the IGSM-WRS runoff model is shown in **Figure 19**. The modeled results show similar overall levels of runoff and patterns of variability to that seen in the observations. Thus, the approach of linking IGSM output to the water system model appear to provide representative projections of runoff for actual river basins.

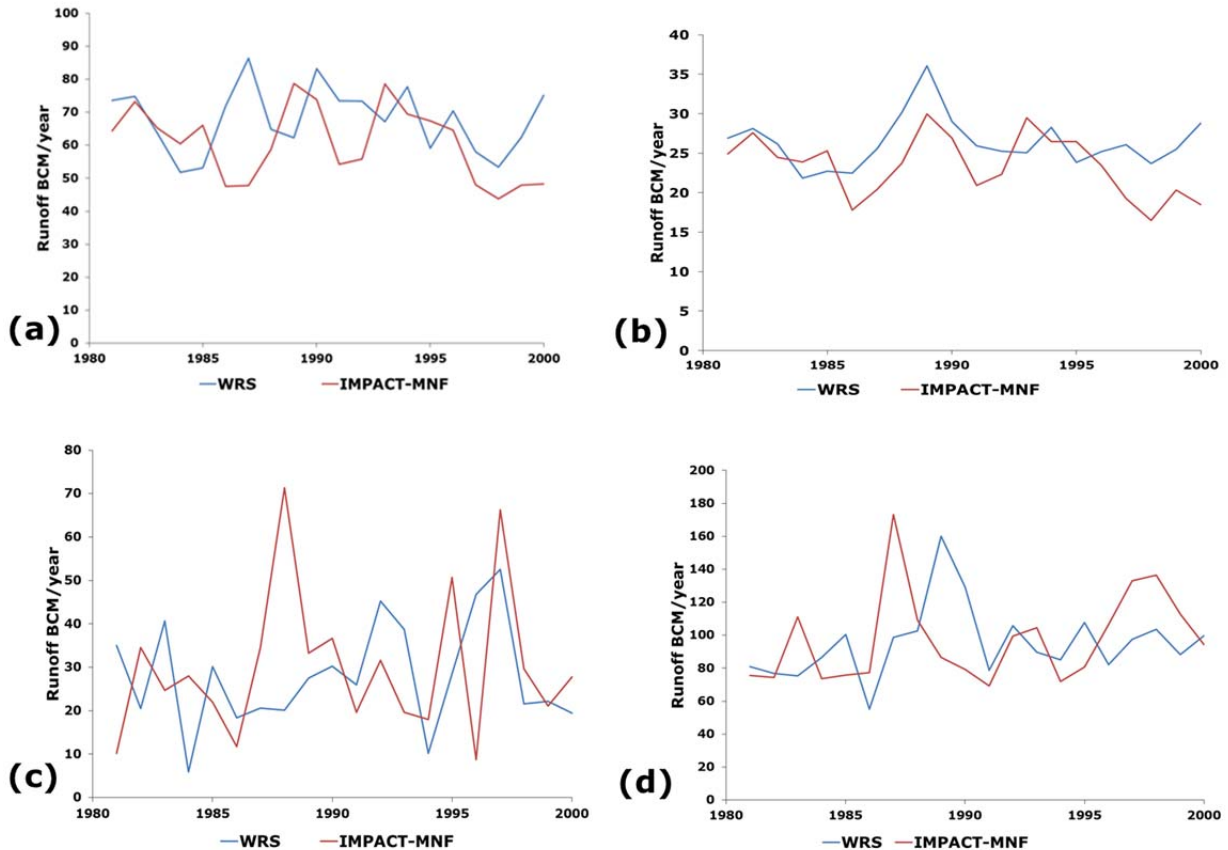


Figure 19. Comparison of the time series of annual natural flow (billion m³) over the period 1981–2000 of IGSM-WRS (blue line) with IFPRI-MNF (red lines) for selected ASRs: (a) Nile-Ethiopia, (b) Nile-Sudan, (c) Murray-Darling, and (d) Missouri.

6.2.2 Water Requirements

Observations for Egypt and Sudan come from FAO AQUASTAT. While the AQUASTAT reports data as a point estimate for 2000, it actually represents conditions averaged over several years up to the reporting year of 2000. For this reason, the AQUASTAT estimates for 2000 are shown with the IGSM-WRS simulated time series for 1980 to 2000. The ASR level results for Murray-Darling come from the Murray-Darling River Basin Authority and for the results for the Missouri Basin from the U.S. Geologic Survey (USGS).

The performance of the IGSM-WRS water requirement components model is shown to be quite good in **Figures 20a-d** for three of the four ASRs. The one ASR that does not perform well is the Missouri River ASR, which is significantly different due to two key factors. One is irrigation: the Missouri basin is extremely large with substantial temperature and precipitation gradients and heterogeneous soils. Irrigation in this ASR is predominately in the Platte River sub-basin of the Missouri where the climate is much hotter and drier than average ASR conditions. This scale issue is addressed in the U.S. version of WRS (Blanc *et al.*, 2012) where the Missouri Basin is divided into 10 sub-basins. The second is thermal electric cooling: The

difference in the non-agricultural withdrawal is that the current global IGSM-WRS does not distinguish between industrial and electric cooling demand.¹¹

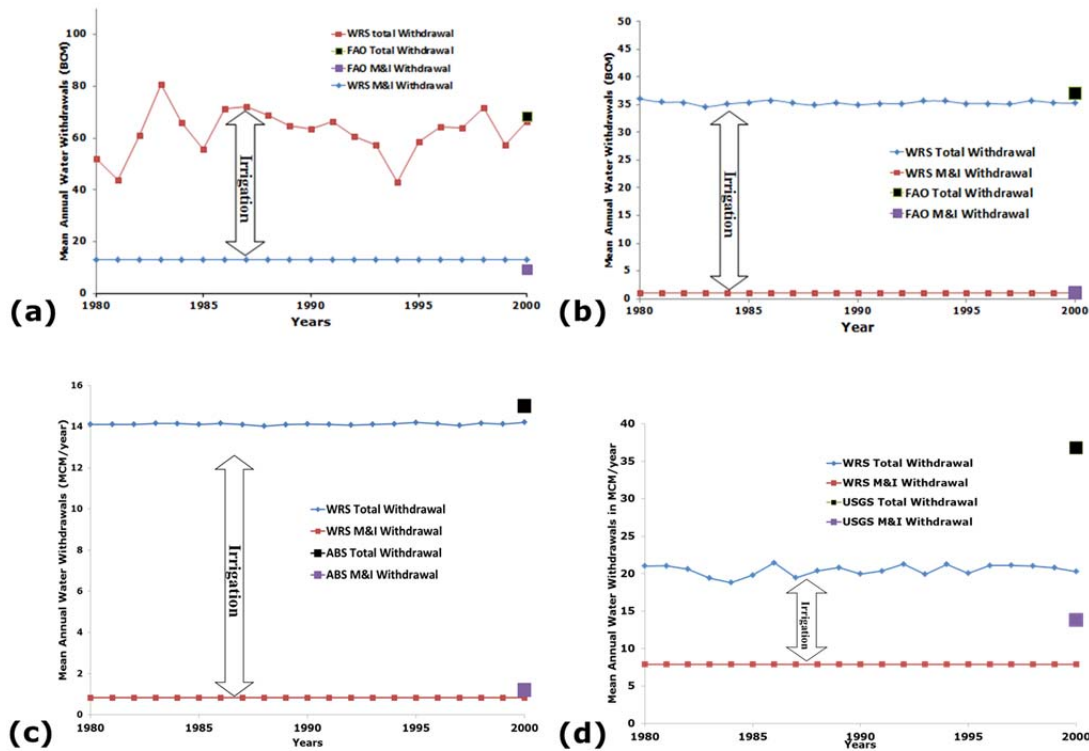


Figure 20. Comparison of annual water withdrawals from IGSM-WRS for the period 1981–2000. Withdrawals for municipal and industrial (M&I, red line), and total (blue line) are shown, and irrigation withdrawals can be seen as the difference between the red and blue lines. Observed data is for 2000 and denoted by a purple square for M&I withdrawals, black square for total withdrawals, and irrigation withdrawal seen as their difference. Results are presented for a selection of ASRs: (a) Nile-Ethiopia [observations from FAO AQUASTAT]; (b) Nile-Sudan [observations from FAO AQUASTAT]; (c) Murray-Darling [observations from Australian Bureau of Statistics (ABS)]; and (d) Missouri [observations from USGS]. Units are billions of m³ in (a) and (b) and millions of m³ in (c) and (d).

6.3 Water Stress

A simple but useful indicator of the state of water systems is water stress. Brown and Matlock (2011) describe a variety of indicators used to estimate water stress. We apply a measure that is used extensively in global water resource assessments, the Water Stress Indicator (WSI) developed by Smakhtin *et al.* (2005).

¹¹ A full model of thermal electric water use, WICTS (Strzepek *et al.*, 2012) is included in the U.S. version of WRS and addresses this issue (Blanc *et al.*, 2012).

Smakhtin *et al.* defines the index as:

$$WSI = \frac{\text{Average Annual Withdrawals}}{\text{Mean Annual Runoff}} \quad (22)$$

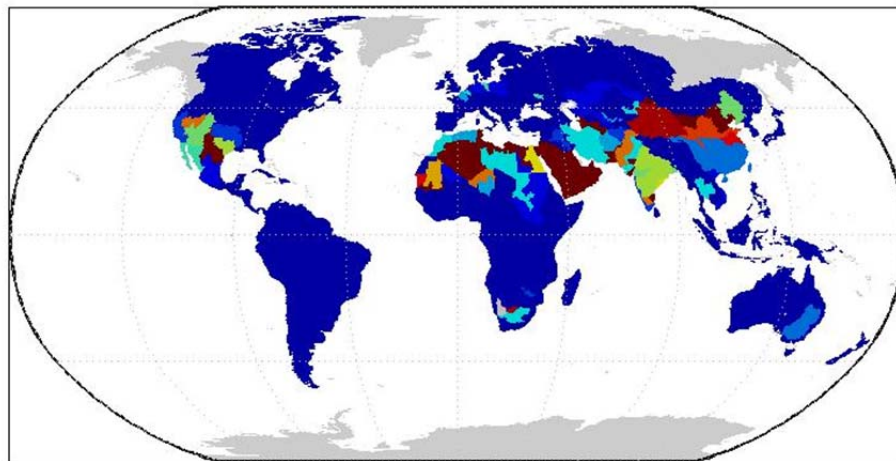
The index is computed over a series of years, and withdrawal is totaled across all sectors representing water demand, and mean annual runoff is used as a proxy for total water availability. Using the notation of the IGSM-WRS this water stress index, computed for each ASR over the period 1981 to 2000, becomes:

$$WSI = \frac{\sum_y \sum_m TWR(m, y)}{\sum_y \sum_m (INF(m, y) + RUN(m, y))} \quad (23)$$

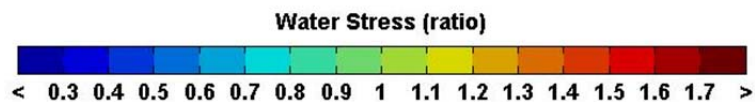
Smakhtin proposes a rough categorization of water stress defined this way, $WSI > 1$ is over exploited, $0.6 > WSI > 1$ is heavily exploited, $0.6 > WSI > 0.3$ is moderately exploited and $WSI < 0.3$ is slightly exploited. The water stress indicators explored here are calculated from inputs to the water management system (Section 2). Similar indices can be computed using the outputs of the ASR operation, such as measures of stress on the irrigation system (e.g., see Blanc *et al.*, 2012).

6.3.1 Global Water Stress

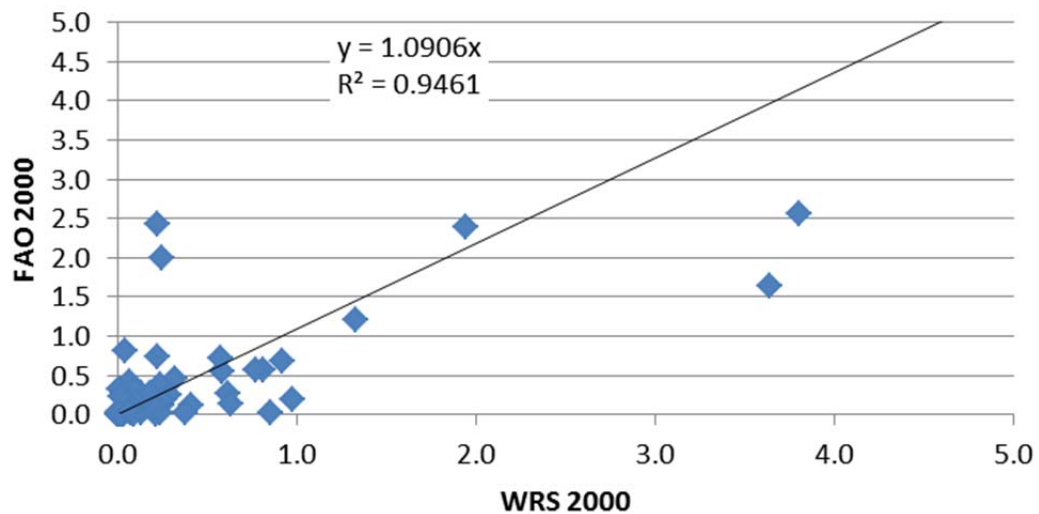
Water Stress results from the IGSM-WRS for the globe using the Smakhtin *et al.* index are shown in **Figure 21a**. The patterns resemble those published in the literature (Brown and Madlock, 2010). **Figure 21b** presents an assessment of the skill of the IGSM-WRS in estimating global water stress by comparing results to FAO-AQUASTAT data. The FAO-AQUASTAT data for 2000 are only reported at the national scale, whereas IGSM-WRS output is by ASR. We therefore aggregate the ARS data to the national level to make this comparison. The figure shows water stress using FAO-AQUASTAT data for 2000 compared with IGSM-WRS results Equation 22) averaged over 1981–2000 because, as discussed earlier, the AQUASTAT data are actually multi-year average, circa the year 2000. Irrigation is the largest water requirement and in ASRs that span large temperature or precipitation gradients, spatial aggregations can lead to biases in irrigation demands as we saw for the Missouri River Basin. Other factors also contribute to differences. In Figure 21b the two points where the IGSM-WRS projects much lower water stress are Lebanon and Turkey, with the difference likely originating in a difference between IGSM-WRS and FAO-AQUASTAT flows. The reason for the other two outliers, Syria and Pakistan, where the IGSM-WRS computes higher water stress appears to be because of differences in irrigation demands, which results from differences in planting dates between the ones assumed in CliCrop and farming practice in these countries.



(a)



Water Stress Comparison



(b)

Figure 21. Results for Water Stress Index (WSI) from the IGSM-WRS averaged over 1981 to 2000 presented as: (a) a map of the 282 ASR annual values (unitless); and (b) scatterplot comparison, by country, of IGSM-WRS WSI and the FAO AQUASTAT WSI, based on observations from the year 2000. Statistics are for a linear regression of AQUASTAT data on WRS estimated values.

6.3.2 ASR Level Water Stress

Water management and impacts occur at the ASR level not the national level. To examine the performance of the IGSM-WRS in estimating water stress, results for the four ASRs explored above are compared with observations as recorded by AQUASTAT, Australian water authorities and the USGS (Figure 22). The categorization of stress is shown by the three colored lines designating the Smakhtin *et al.* categories described above. For the Nile-Ethiopia, Murray-Darling and Missouri the IGSM-WRS results are very close to observations. For the Nile-Sudan IGSM-WRS underestimates the stress index because the local Nile flows in Sudan include the very complex Sudd wetlands and IGSM-WRS estimates higher internal Sudan Nile runoff than FAO reports. Additionally, irrigation is the predominant sectoral water withdrawal and differences are found between irrigation demand estimated with IGSM-WRS and what is reported in AQUASTAT. While there is difference in the water stress index between the IGSM-WRS based value and the AQUASTAT based value, both estimates find that the Nile-Sudan falls in the over-exploited water stress classification. This classification warns that there is extreme human pressure on the water resource in this region.

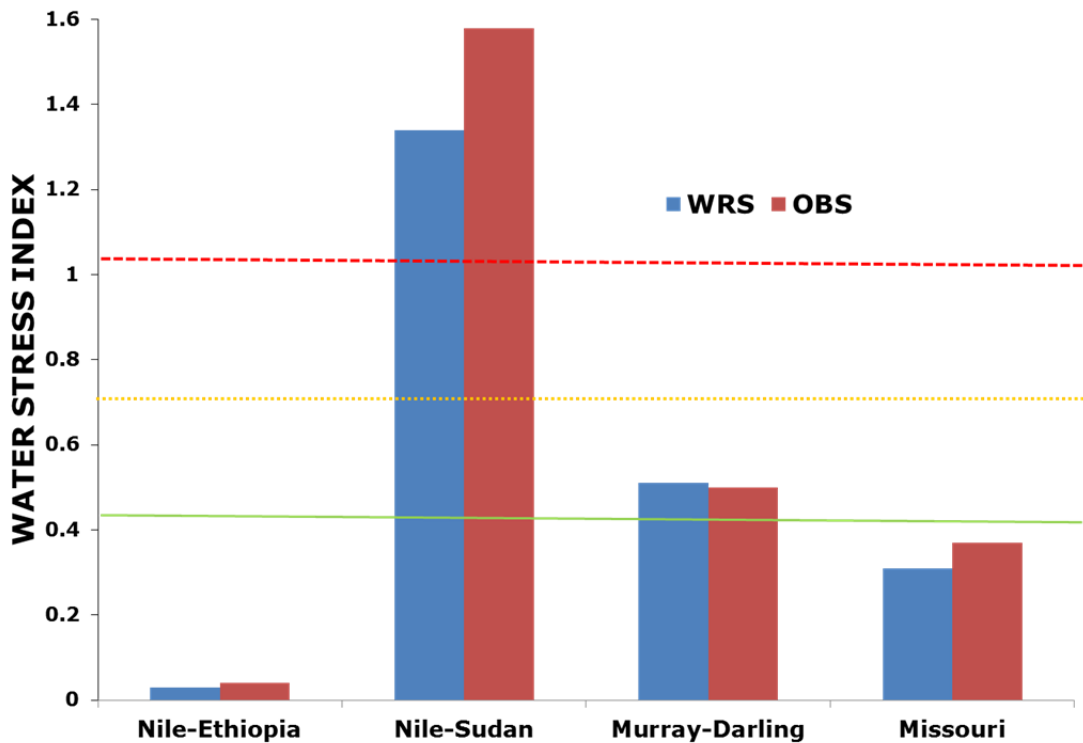


Figure 22. Comparison of Water Stress Index (WSI, unitless) from IGSM-WRS mean over simulation years 1981–2000 (blue bars) with observed data for 2000 (red bars). Results are provided for selected ASRs: Nile-Ethiopia (observations based on FAO AQUASTAT); Nile-Sudan (observations based on FAO AQUASTAT); Murray-Darling (from Murray-Darling Basin Authority); and Missouri (observations from USGS). Colored lines show Smakhtin stress categories.

7. SUMMARY AND APPLICATIONS

The Water Resource Systems framework presented here is a significant step forward in linking together a numerically efficient model that represents the economic, hydrologic and climatological determinants of the performance of water resource systems. It provides a useful tool for assessment of conflicts between alternative water uses as they may evolve with future population and economic growth, considering the effects on water supply of climate change. Schlosser *et al.*, (2012) have applied the model to assessment of the effects of projected climate change at the 282 ASR level, applying the model specification presented here. Effects on water systems are explored under climate change to 2100 according to two different climate models under a no-new-policy reference case and policies limiting atmospheric GHG concentrations to 450 ppm CO₂-e. Blanc *et al.* (2012) apply the model to a 99 ASR specification of the continental U.S., imposing changes in characterizations of water requirements made possible by more complete data inputs for this particular region. The same two policy scenarios, and two climate models are employed and a number of measures of system stress and adequacy are studied.

In putting together a global modeling system, the need for computational efficiency and data limits leads to inevitable compromises. Even with these compromises this system provides a tool for screening for regions where water stresses may arise, providing global coverage. For detailed evaluation and resource planning for an individual river basin, a more detailed model would be needed. In that regard, the IGSM-WRS provides a framework where detail and resolution can be added where data is available and where resources are available to carry out improvements.

Acknowledgments

The Joint Program on the Science and Policy of Global Change is funded by the U.S. Department of Energy, Office of Science under grants DE-FG02-94ER61937, DE-FG02-93ER61677, DE-FG02-08ER64597, and DE-FG02-06ER64320; the U.S. Environmental Protection Agency under grants XA-83344601-0, XA-83240101, XA-83042801-0, PI-83412601-0, RD-83096001, and RD-83427901-0; the U.S. National Science Foundation under grants SES-0825915, EFRI-0835414, ATM-0120468, BCS-0410344, ATM-0329759, and DMS-0426845; the U.S. National Aeronautics and Space Administration under grants NNX07AI49G, NNX08AY59A, NNX06AC30A, NNX09AK26G, NNX08AL73G, NNX09AI26G, NNG04GJ80G, NNG04GP30G, and NNA06CN09A; the U.S. National Oceanic and Atmospheric Administration under grants DG1330-05-CN-1308, NA070AR4310050, and NA16GP2290; the U.S. Federal Aviation Administration under grant 06-C-NE-MIT; the Electric Power Research Institute under grant EP-P32616/C15124; and a consortium of 40 industrial and foundation sponsors (for the complete list see <http://globalchange.mit.edu/sponsors/current.html>).

8. REFERENCES

- Alder, R.F., G.J. Huffman, A. Chang, R. Ferraro, P.-P. Xie, J. Janowiak, B. Rudolf, U. Schneider, S. Curtis, D. Bolvin, A. Gruber, J. Susskind, P. Arkin and E. Nelkin, 2003: The version-2 global precipitation climatology project (GPCP) monthly precipitation analysis (1979–present). *Journal of Hydrometeorology*, 4: 1147–1167.
- Allen, R.G., L.S. Pereira, D. Raes and M. Smith, 1998: Crop evapotranspiration: Guidelines for computing crop requirements. *Irrigation and Drainage Paper*, 56, Food and Agriculture Organization (FAO): Rome, Italy.
- Alcamo, J., P. Döll, T. Henrichs, F. Kaspar, B. Lehner, T. Rösch, S. Siebert, 2003: Development and Testing of the Water GAP 2 Global Model of Water Use and Availability. *Hydrological Science*, 48(3): 317–333.
- Blanc *et al.*, 2012: Global Change impacts on Water Stress in the United States. MIT JPSPGC Report forthcoming.
- Brown, A. and M.D. Matlock, 2011: A Review of Water Scarcity Indices and Methodologies. University of Arkansas, the Sustainability Consortium White Paper, 106.
- CGIAR [Consultative Group on International Agricultural Research], 2012: *The Global Potential Evapo-Transpiration (Global-PET) and Global Aridity Index (Global-Aridity)* (<http://www.cgiar-csi.org/data/global-aridity-and-pet-database>).
- Cole, M.A., 2004: Economic Growth and Water Use. *Applied Economics Letters*, 11: 1–4.
- Cosgrove, W. and F.R. Rijsberman, 2000: *World water vision: making water everybody's business*. EarthScan Publishing, Ltd.: London, UK, pp. 136.
- FAO, 2012: AQUASTAT (<http://www.fao.org/nr/water/aquastat/main/index.stm>).
- FAO, 2010: CROPWAT 8.0 (http://www.fao.org/nr/water/infores_databases_cropwat.html).
- FAO-UNESCO, 2005: *Soil Map of the World, digitized by ESRI. Soil climate map*, USDA-NRCS, Soil Survey Division, World Soil Resources: Washington, D.C. (<http://soils.usda.gov/use/worldsoils/mapindex/order.html>).
- Fant, C., A. Gueneau, K. Strzepek, S. Awadalla, W. Farmer, É. Blanc and C. Schlosser, 2012: CliCrop: A Water-Stress and Irrigation Demand Model for an Integrated Global Assessment Modeling Approach, MIT JPSPGC Report 214, April, 26 p. (http://globalchange.mit.edu/files/document/MITJPSPGC_Rpt214.pdf).
- Farmer, W. 2011: *Estimating Monthly Time Series of Streamflows at Ungauged Locations in the United States*, Master of Science Thesis in Environmental and Water Resources Engineering, Tufts University Department of Civil and Environmental Engineering, Medford, Massachusetts, November.
- Fekete, B.M., C.J. Vörösmarty and W. Grabs 2002: High Resolution Fields of Global Runoff Combining Observed River Discharge and Simulated Water Balances, *Global Biogeochemical Cycles*, 16(3) (<http://dx.doi.org/10.1029/1999GB001254>).
- Fischer, 2012: GAEZ v3.0 Global Agro-ecological Zones. IIASA/FAO (<http://www.gaez.iiasa.ac.at>).
- Gangopadhyay, S.W., F.R. Cosgrove, Rijsberman, and K. Strzepek, 2001: The World Water Vision: From Developing a Vision to Action. *American Geophysical Union*, Spring Meeting, Abstract H22E-04.

- Gueneau, A., 2012: *Crop Water Stress under Climate Change Uncertainty: Global Policy and Regional Risk*, Master of Science Thesis in Technology and Policy, Massachusetts Institute of Technology, June.
- Hirsch, R.M., 1982: A comparison of four streamflow record extension techniques, *Water Resource Res.* 18: 1081–1088.
- Keller A.A. and J. Keller, 1995: Effective Efficiency: A Water Use Efficiency Concept for Allocating Freshwater Resources. 1995. 20 p. *Center for Economic Policy Studies*, Discussion Paper 22, Winrock International: Arlington VA.
- Keller, A., J. Keller and D. Seckler, 1995: *Integrated water resource systems: theory and policy implications*. International Irrigation Management Institute: Colombo, Sri Lanka.
- Kenny, J.F., N.L. Barber, S.S. Hutson, K.S. Linsey, J.K. Lovelace and M.A. Maupin, 2009: Estimated Use of Water in the United States in 2005. *United States Geological Survey (USGS) Circular*, 1344, USGS: Reston, VA.
- Lawrence, D., K.W. Oleson, M.G. Flanner, P.E. Thornton, S.C. Swenson, P.J. Lawrence, X. Zeng, Z.-L. Yang, S. Levis, K. Skaguchi, G.B. Bonan and A.G. Slater, 2011: Parameterization Improvements and Functional and Structural Advances in Version 4 of the Community Land Model. *J. Adv. Model. Earth Syst.*, 3(1): doi:10.1029/JAMES.2011.3.1.
- Maurer, E.P., 2007: Uncertainty in hydrologic impacts of climate change in the Sierra Nevada, California under two emissions scenarios. *Climatic Change*, 82: doi: 10.1007/s10584-006-9180-9.
- McMahon, T.A., R.M. Vogel, M.C. Peel, G.G.S. Pegram, 2007: Global streamflows – Part 1: characteristics of annual streamflows. *Journal of Hydrology*, 347(3–4): 243–259.
- Meehl, G.A., C. Covey, T. Delworth, M. Latif, B. McAvaney, J.F.B. Mitchell, R.J. Stouffer and K.E. Taylor, 2007: The WCRP CMIP3 multi-model dataset: A new era in climate change research. *Bull. Amer. Met. Soc.*, 88: 1383–1394.
- Milly, P.C.D., J. Betancourt, M. Falkenmark, R.M. Hirsch, W. Z.W. Kundzewicz, D.P. Lettenmaier and R.J. Stouffer, 2008: Stationarity Is Dead: Whither Water Management? *Science*, 319: 2008.02.01.
- Milly P, K. Dunne and A. Vecchia, 2005: Global pattern of trends in streamflow and water availability in a changing climate. *Nature*, 438: 347–350.
- Mitchell, T.D. and P.D. Jones, 2005: An improved method of constructing a database of monthly climate observations and associated high-resolution grids. *International Journal of Climatology*, 25: 693–712.
- Neitsch, S.L., J.G. Arnold, J.R. Kiniry and S.R. Williams, 2002: Soil and Water Assessment Tool User's Manual Version 2000. *GSWRL Report 02-02*, BRC Report 02-06. Texas Water Resources Institute TR-192: College Station, TX, pp. 438.
- Oleson, K.W., Y. Dai, G. Bonan, M. Bosilovich, R. Dickinson, P. Dirmeyer, F. Hoffman, P. Houser, S. Levis, G.-Y. Niu, P. Thornton, M. Vertenstein, Z.-L. Yang and X. Zeng, 2004: *Technical description of the Community Land Model (CLM)*. National Center for Atmospheric Research *Tech. Note NCAR/TN-461+STR*, 173 pp.
- Paltsev, S., J.M. Reilly, H.D. Jacoby, R.S. Eckaus, J. McFarland, M. Sarofim, M. Asadoorian and M. Babiker 2005: The MIT Emissions Prediction and Policy Analysis (EPPA) Model:

- Version 4, MIT JPSPGC *Report 125*, August, 72 p.
[\(\[http://web.mit.edu/globalchange/www/MITJPSPGC_Rpt125.pdf\]\(http://web.mit.edu/globalchange/www/MITJPSPGC_Rpt125.pdf\)\)](http://web.mit.edu/globalchange/www/MITJPSPGC_Rpt125.pdf).
- Raskin, P., G. Gallopin, P. Gutman, A. Hammond and R. Swart, 1998: Bending the Curve: Toward Global Sustainability. A report of the Global Scenario Group, *PoleStar Series Report 8*, Stockholm Environment Institute: Sweden, 38 p.
- Raskin, P., P.H. Gleick, P. Kirshen, R.G. Pontius, Jr. and K. Strzepek, 1997: Comprehensive assessment of the freshwater resources of the world. Document prepared for UN Commission for Sustainable Development 5th Sessio. Stockholm Environmental Institute, Sweden.
- Rosengrant, M., C. Ringler, S. Msangi, T. Sulser, T. Zhu and S. Cline 2008: International Model for Policy Analysis of Agricultural Commodities and Trade (IMPACT): Model Description, International Food Research Institute: Washington, D.C.
- Sacks, W.J., D. Deryng, J.A. Foley and N. Ramankutty, 2010: Crop planting dates: An analysis of global patterns. Submitted to and accepted by *Global Ecology and Biogeography*.
- Schlosser, C.A., D. Kicklighter and A. Sokolov, 2007: A Global Land System Framework for Integrated Climate-Change Assessments, MIT JPSPGC *Report 147*, May, 60 p.
[\(\[http://web.mit.edu/globalchange/www/MITJPSPGC_Rpt147.pdf\]\(http://web.mit.edu/globalchange/www/MITJPSPGC_Rpt147.pdf\)\)](http://web.mit.edu/globalchange/www/MITJPSPGC_Rpt147.pdf).
- Schlosser, C.A., X. Gao, K. Strzepek, A. Sokolov, C.E. Forest, S. Awadalla, and W. Farmer, 2012: Quantifying the likelihood of regional climate change: A hybridized approach, *J. Climate*, (accepted).
- Schlosser *et al.*, 2012: Global Change impacts on Global Water Stress MIT JPSPGC *Report forthcoming*.
- Sokolov, A., P. Stone, C. Forest, R. Prinn, M. Sarofim, M. Webster, S. Paltsev, C. Schlosser, D. Kicklighter, S. Dutkiewicz, J. Reilly, C. Wang, B. Felzer, J. Melillo and H. Jacoby 2009: Probabilistic Forecast for 21st Century Climate Based on Uncertainties in Emissions (without Policy) and Climate Parameters. *Journal of Climate*, 22(19): 5175–5204.
- Sokolov, A.P., C.A. Schlosser, S. Dutkiewicz, S. Paltsev, D.W. Kicklighter, H.D. Jacoby, R.G. Prinn, C.E. Forest, J.M. Reilly, C. Wang, B. Felzer, M.C. Sarofim, J. Scott, P.H. Stone, J.M. Melillo and J. Cohen, 2007: A Global Land System Framework for Integrated Climate-Change Assessments, MIT JPSPGC *Report 124*, July, 40 p.
[\(\[http://web.mit.edu/globalchange/www/MITJPSPGC_Rpt124.pdf\]\(http://web.mit.edu/globalchange/www/MITJPSPGC_Rpt124.pdf\)\)](http://web.mit.edu/globalchange/www/MITJPSPGC_Rpt124.pdf).
- Smakhtin, V., 2008: Basin Closure and Environmental Flow Requirements. *Water Resources Development*, 24(2): 227–33.
- Smakhtin, V., C. Revenga, and P. Döll, 2004a: A Pilot Global Assessment of Environmental Water Requirements and Scarcity. *Water International*, 29(3): 307–317.
- Strzepek, K., J. Baker, W. Farmer, and C.A. Schlosser 2012: Modeling Water Withdrawal and Consumption for Electricity Generation in the United States MIT JPSPGC *Report 222*, June 2012, p.46. [\(\[http://globalchange.mit.edu/files/document/MITJPSPGC_Rpt222.pdf\]\(http://globalchange.mit.edu/files/document/MITJPSPGC_Rpt222.pdf\)\)](http://globalchange.mit.edu/files/document/MITJPSPGC_Rpt222.pdf).
- UNEP, 2008: VITAL WATER GRAPHICS: An Overview of the State of the World’s Fresh and Marine Waters— 2nd Edition, 2008. [\(<http://www.unep.org/dewa/vitalwater/index.html>\)](http://www.unep.org/dewa/vitalwater/index.html).
- USGS 2012: Water Use in the United States (<http://water.usgs.gov/watuse>).
- (WMO, 2012) Global Runoff Data Centre (http://www.bafg.de/mn_266918/GRDC/EN/Home/).

- Webster, M.D., A.P. Sokolov, J.M. Reilly, C. Forest, S. Paltsev, C.A. Schlosser, C. Wang, D.W. Kicklighter, M. Sarofim, J.M. Melillo, R.G. Prinn and H.D. Jacoby 2012: Analysis of climate policy targets under uncertainty. *Climatic Change*, 112(3–4) 569–583.
- Zhu, T., C. Ringler and M.W. Rosegrant, 2012: Development and testing of a global hydrological model for integrated assessment modeling. Working Paper, *International Food Policy Research Institute*: Washington, DC.

Appendix

Table 1. Mapping of EPPA regions to WRS spatial units of analysis

EPPA Region	WRS REGION	Assessment SubRegion (ASR)
Africa	Algeria	North African Coast Algeria
		Sahara Algeria
	Angola	Central African West Coast Angola
		Congo Angola
		Zambezi Angola
	Benin	Niger Benin
		Volta Benin
	Botswana	Kalahari Botswana
		Limpopo Botswana
		Zambezi Botswana
	Burkina Faso	Niger Burkina Faso
		Volta Burkina Faso
	Burundi	East African Coast Burundi
		Cameroon
	Lake Chad Basin Cameroon	
	Niger Cameroon	
	Central African Republic	Central African Central African Republic
		Congo Central African Republic
		Lake Chad Basin Central African Republic
	Chad	Lake Chad Basin Chad
		Niger Chad
		Sahara Chad
	Congo	Central African West Coast Congo
		Congo Congo
	Djibouti	Nile Djibouti
	DRC	Congo DRC
		East African Coast DRC
		Zambezi DRC
	Egypt	Eastern Mediterranean Egypt
		Nile Egypt
North African West Coast Egypt		
Equatorial Guinea	Sahara Egypt	
	Central African West Coast Equatorial Guinea	
Eritrea	Nile Eritrea	
Ethiopia	Horn of Africa Ethiopia	
	Nile Ethiopia	
Gabon	Central African Gabon	

EPPA Region	WRS REGION	Assessment SubRegion (ASR)
	Gambia	West African Coast Gambia
	Ghana	Volta Ghana
	Guinea	Senegal Guinea
		Niger Guinea
		West African Coast Guinea
	Guinea Bissau	West African Coast Guinea Bissau
	Ivory Coast	Volta Ivory Coast
		West African Coast Ivory Coast
		Niger Ivory Coast
	Kenya	Horn of Africa Kenya
	Lesotho	Orange Lesotho
	Liberia	West African Coast Liberia
	Libya	North African Coast Libya
		Sahara Libya
	Madagascar	Madagascar Madagascar
	Malawi	Zambezi Malawi
	Mali	Niger Mali
		Sahara Mali
		Senegal Mali
		Volta Mali
	Mauritania	Northwest Africa Mauritania
		Sahara Mauritania
		Senegal Mauritania
	Morocco	Northwest Africa Morocco
		Sahara Morocco
	Mozambique	Limpopo Mozambique
		Southeast Africa Mozambique
		Zambezi Mozambique
	Namibia	Central African West Coast Namibia
		Kalahari Namibia
		Orange Namibia
		Zambezi Namibia
	Niger	Lake Chad Basin Niger
		Niger Niger
		Sahara Niger
	Nigeria	Lake Chad Basin Nigeria
		Niger Nigeria
	Rwanda	East African Coast Rwanda
	Senegal	Senegal Senegal
		West African Coast Senegal
	Sierra Leone	West African Coast Sierra Leone
	Somalia	Horn of Africa Somalia

EPPA Region	WRS REGION	Assessment SubRegion (ASR)
	South Africa	Kalahari South Africa
		Orange South Africa
		South African Coast South Africa
	Sudan	Nile Sudan
		Sahara Sudan
	Swaziland	South African Coast Swaziland
	Tanzania	East African Coast Tanzania
		Southeast Africa Tanzania
		Zambezi Tanzania
	Togo	Volta Togo
	Tunisia	North African Coast Tunisia
	Uganda	East African Coast Uganda
		Horn of Africa Uganda
		Nile Uganda
	Vietnam	Northwest Africa Morocco
	Zambia	Zambezi Zambia
	Zimbabwe	Limpopo Zimbabwe
		Southeast Africa Zimbabwe
		Zambezi Zimbabwe
Australia & New Zealand	Australia	Central Australia Australia
		Eastern Australia Australia
		Murray Australia Australia
		Western Australia Australia
	New Zealand	New Zealand New Zealand
Higher Income East Asia	Malaysia	Borneo Malaysia
		Thai-Myan-Malay Malaysia
	Philippines	Philippines Philippines
	Singapore	Thai-Myan-Malay Singapore
	South Korea	South Korea Peninsula South Korea
	Thailand	Mekong Thailand
		Thai-Myan-Malay Thailand
Canada	Canada	Canada Arctic Canada
		Central Canada Slave Basin Canada
		Columbia Canada
		Great Lakes Canada
		Red Winnipeg Canada
China	China	Amur China
		Brahmaputra China
		Chang Jiang China
		Ganges China

EPPA Region	WRS REGION	Assessment SubRegion (ASR)
		Hail He China
		Hual He China
		Huang He China
		Indus China
		Langcang Jiang China
		Lower Mongolia China
		Ob China
		Southeast Asian Coast China
		Songhua China
		Yili He China
		Zhu Jiang China
Eastern Europe	Central Europe	Danube Central Europe
	Poland	Oder Poland
European Union	Alpine Europe	Danube Alpine Europe
		Rhine Alpine Europe
	Belgium Luxembourg	Rhine Belgium Luxembourg
	Scandinavia	Scandinavia Scandinavia
		Elbe Scandinavia
	France	Loire Bordeaux France
		Rhine France
		Rhone France
		Seine France
	Germany	Danube Germany
		Elbe Germany
		Oder Germany
		Rhine Germany
	British Isles	Britain British Isles
		Ireland British Isles
	Italy	Italy Italy
	Netherlands	Rhine Netherlands
	Iberia	Iberia East Mediterranean Iberia
		Iberia West Atlantic Iberia
Former Soviet Union	Caucus	Black Sea Caucasus
	Baltic	Dnieper Baltic
		Baltic Baltic
	Kazakhstan	Volga Kazakhstan
		Yili He Kazakhstan
		Ural Kazakhstan
		Syrdarja Kazakhstan
		Ob Kazakhstan
		Lake Balkhash Kazakhstan

EPPA Region	WRS REGION	Assessment SubRegion (ASRs)
		Amudarja Kazakhstan
	Kyrgyzstan	Syrdarja Kyrgyzstan
		Lake Balkhash Kyrgyzstan
	Russia	Baltic Russia
		Black Sea Russia
		Dnieper Russia
		Oder Russia
		Amur Russia
		Northern Europe Russia Russia
		Ob Russia
		Upper Mongolia Russia
		Ural Russia
		Volga Russia
		Yenisey Russia
	Tajikistan	Amudarja Tajikistan
	Turkmenistan	Amudarja Turkmenistan
		Ural Turkmenistan
		Western Asia Ira Turkmenistan
	Ukraine	Black Sea Ukraine
		Danube Ukraine
		Dnieper Ukraine
	Uzbekistan	Amudarja Uzbekistan
		Syrdarja Uzbekistan
Indonesia	Indonesia	Borneo Indonesia
		Indonesia East Indonesia
		Indonesia West Indonesia
India	India	Brahmaputra India
		Brahmari India
		Cauvery India
		Chotanagpui India
		Eastern Ghats India
		Ganges India
		Godavari India
		India East Coast India
		Indus India
		Krishna India
		Langcang Jiang India
		Luni India
		Mahi Tapti India
		Sahyada India
Japan	Japan	Japan Japan
Latin America	Argentina	Parana Argentina

EPPA Region	WRS REGION	Assessment SubRegion (ASRs)
		Rio Colorado Argentina
		Salada Tierra Argentina
		Tierra Argentina
	Brazil	Amazon Brazil
		Northeast Brazil Brazil
		Parana Brazil
		San Francisco Brazil
		Toc Brazil
		Uruguay Brazil
	Caribbean Central America	Yucatan Caribbean Central America
		Central America Caribbean Central America
		Cuba Caribbean Central America
		Caribbean Caribbean Central America
	Central South America	Amazon Central South America
		Parana Central South America
	Chile	Chile Coast Chile
	Colombia	Northwest South Colombia
		Orinoco Colombia
		Amazon Colombia
	Ecuador	Amazon Ecuador
		Northwest South Ecuador
	Northern South America	Northern South America Northern South America
		Orinoco Northern South America
	Peru	Amazon Peru
		Peru Coastal Peru
	Uruguay	Uruguay Uruguay
Middle East States	Iran	Tigris Euphrates Iran
		Western Asia Iran Iran
	Iraq	Arabian Peninsula Iraq
		Tigris Euphrates Iraq
	Israel	Eastern Mediterranean Israel
	Jordan	Eastern Mediterranean Jordan
	Gulf	Arabian Peninsula Gulf
	Lebanon	Eastern Mediterranean Lebanon
	Syria	Eastern Mediterranean Syria
		Tigris Euphrates Syria
Mexico	Mexico	Middle Mexico Mexico
		Rio Grande Mexico
		Upper Mexico Mexico

EPPA Region	WRS REGION	Assessment SubRegion (ASR)
		Yucatan Mexico
Rest of World	Afghanistan	Amudarja Afghanistan
		Western Asia Iran Afghanistan
	Bangladesh	Brahmaputra Bangladesh
		Ganges Bangladesh
		Thai-Myan-Malay Bangladesh
	Bhutan	Brahmaputra Bhutan
	Southeast Asia	Mekong Southeast Asia
	Cyprus	Eastern Mediterranean Cyprus
	North Korea	North Korea Peninsula North Korea
	Mongolia	Lower Mongolia Mongolia
		Upper Mongolia Mongolia
	Myanmar	Mekong Myanmar
		Thai-Myan-Malay Myanmar
	Nepal	Ganges Nepal
	Pakistan	Indus Pakistan
		Western Asia Iran Pakistan
	Papua New Guinea	Papua Oceania Papua New Guinea
	Sri Lanka	Sri Lanka Sri Lanka
	Turkey	Black Sea Turkey
		Danube Turkey
		Eastern Med Turkey
		Tigris Euphrates Turkey
	Vietnam	Southeast Asian Coast Vietnam
	Adriatic	Danube Adriatic
	ROW	ROW ROW
United States	United States	Arkansas United States
		California United States
		Colorado United States
		Columbia United States
		Great Basin United States
		Great Lakes United States
		Mississippi United States
		Missouri United States
		Ohio United States
		Red Winnipeg United States
		Rio Grande United States
		Southeast U.S. United States
		U.S. Northeast United States
		Western Gulf Mexico United States

Table A2. River basins and regional hydrologic units.

Amazon	Amudarja	Amur
Arabian Peninsula	Arkansas	Baltic
Black Sea	Borneo	Brahmaputra
Brahmari	Britain	California
Canada-Arctic-Atlantic	Caribbean	Cauvery
Central African West Coast	Central America	Central Australia
Central Canada Slave Basin	Chang Jiang	Chotanagpul
Colorado	Columbia	Columbia Ecuador
Congo	Cuba	Danube
Dnieper	East African Coast	Eastern Ghats
Eastern Australia Tasmania	Eastern Mediterranean	Elbe
Ganges	Godavari	Great Basin
Great Lakes	Hai He	Horn of Africa
Hua He	Huang He	Iberia East Mediterranean
Iberia West Atlantic	India East Coast	Indonesia East
Indonesia West	Indus	Ireland
Italy	Japan	Kalahari
Krishna	Lake Balkhash	Lake Chad Basin
Langcang Jiang	Limpopo	Loire-Bordeaux
Lower Mongolia	Luni	Madagascar
Mahi Tapti	Mekong	Middle Mexico
Mississippi	Missouri	Murray Australia
New Zealand	Niger	Nile
North African Coast	North Euro Russia	North Korea Peninsula
North South America	Northeast Brazil	Northwest Africa
Northwest South America	Ob	Oder
Ohio	Orange	Orinoco
Papua Oceania	Parana	Peru Coastal
Philippines	Red-Winnipeg	Rhine
Rhone	Rio Colorado	Rio Grande
Rest-of-World (ROW)	Sahara	Sahyada
Salada Tierra	San Francisco	Scandinavia
Southeast Asian Coast	Seine	Senegal
Songhua	South African Coast	South Korean Peninsula
Southeast African Coast	Southeast U.S.	Sri Lanka
Syrdarja	Thai-Myan-Malay	Tierra
Tigris-Euphrates	Toc	Upper Mexico
Upper Mongolia	Ural	Uruguay
US Northeast	Volga	Volta
West African Coastal	Western Asia-Iran	Western Australia
Western Gulf Mexico	Yenisey	Yili He
Yucatan	Zambezi	Zhu Jian

REPORT SERIES of the MIT Joint Program on the Science and Policy of Global Change

FOR THE COMPLETE LIST OF JOINT PROGRAM REPORTS:
<http://globalchange.mit.edu/pubs/all-reports.php>

192. **The Impact of Border Carbon Adjustments under Alternative Producer Responses** *Winchester* February 2011
193. **What to Expect from Sectoral Trading: A U.S.-China Example** *Gavard et al.* February 2011
194. **General Equilibrium, Electricity Generation Technologies and the Cost of Carbon** *Abatement Lanz and Rausch* February 2011
195. **A Method for Calculating Reference Evapotranspiration on Daily Time Scales** *Farmer et al.* February 2011
196. **Health Damages from Air Pollution in China** *Matus et al.* March 2011
197. **The Prospects for Coal-to-Liquid Conversion: A General Equilibrium Analysis** *Chen et al.* May 2011
198. **The Impact of Climate Policy on U.S. Aviation** *Winchester et al.* May 2011
199. **Future Yield Growth: What Evidence from Historical Data** *Gitiaux et al.* May 2011
200. **A Strategy for a Global Observing System for Verification of National Greenhouse Gas Emissions** *Prinn et al.* June 2011
201. **Russia's Natural Gas Export Potential up to 2050** *Paltsev* July 2011
202. **Distributional Impacts of Carbon Pricing: A General Equilibrium Approach with Micro-Data for Households** *Rausch et al.* July 2011
203. **Global Aerosol Health Impacts: Quantifying Uncertainties** *Selin et al.* August 2011
204. **Implementation of a Cloud Radiative Adjustment Method to Change the Climate Sensitivity of CAM3** *Sokolov and Monier* September 2011
205. **Quantifying the Likelihood of Regional Climate Change: A Hybridized Approach** *Schlosser et al.* October 2011
206. **Process Modeling of Global Soil Nitrous Oxide Emissions** *Saikawa et al.* October 2011
207. **The Influence of Shale Gas on U.S. Energy and Environmental Policy** *Jacoby et al.* November 2011
208. **Influence of Air Quality Model Resolution on Uncertainty Associated with Health Impacts** *Thompson and Selin* December 2011
209. **Characterization of Wind Power Resource in the United States and its Intermittency** *Gunturu and Schlosser* December 2011
210. **Potential Direct and Indirect Effects of Global Cellulosic Biofuel Production on Greenhouse Gas Fluxes from Future Land-use Change** *Kicklighter et al.* March 2012
211. **Emissions Pricing to Stabilize Global Climate** *Bosetti et al.* March 2012
212. **Effects of Nitrogen Limitation on Hydrological Processes in CLM4-CN** *Lee & Felzer* March 2012
213. **City-Size Distribution as a Function of Socio-economic Conditions: An Eclectic Approach to Down-scaling Global Population** *Nam & Reilly* March 2012
214. **CliCrop: a Crop Water-Stress and Irrigation Demand Model for an Integrated Global Assessment Modeling Approach** *Fant et al.* April 2012
215. **The Role of China in Mitigating Climate Change** *Paltsev et al.* April 2012
216. **Applying Engineering and Fleet Detail to Represent Passenger Vehicle Transport in a Computable General Equilibrium Model** *Karplus et al.* April 2012
217. **Combining a New Vehicle Fuel Economy Standard with a Cap-and-Trade Policy: Energy and Economic Impact in the United States** *Karplus et al.* April 2012
218. **Permafrost, Lakes, and Climate-Warming Methane Feedback: What is the Worst We Can Expect?** *Gao et al.* May 2012
219. **Valuing Climate Impacts in Integrated Assessment Models: The MIT IGSM** *Reilly et al.* May 2012
220. **Leakage from Sub-national Climate Initiatives: The Case of California** *Caron et al.* May 2012
221. **Green Growth and the Efficient Use of Natural Resources** *Reilly* June 2012
222. **Modeling Water Withdrawal and Consumption for Electricity Generation in the United States** *Strzepek et al.* June 2012
223. **An Integrated Assessment Framework for Uncertainty Studies in Global and Regional Climate Change: The MIT IGSM** *Monier et al.* June 2012
224. **Cap-and-Trade Climate Policies with Price-Regulated Industries: How Costly are Free Allowances?** *Lanz and Rausch* July 2012.
225. **Distributional and Efficiency Impacts of Clean and Renewable Energy Standards for Electricity** *Rausch and Mowers* July 2012.
226. **The Economic, Energy, and GHG Emissions Impacts of Proposed 2017–2025 Vehicle Fuel Economy Standards in the United States** *Karplus and Paltsev* July 2012
227. **Impacts of Land-Use and Biofuels Policy on Climate: Temperature and Localized Impacts** *Hallgren et al.* August 2012
228. **Carbon Tax Revenue and the Budget Deficit: A Win-Win-Win Solution?** *Sebastian Rausch and John Reilly* August 2012
229. **CLM-AG: An Agriculture Module for the Community Land Model version 3.5** *Gueneau et al.* September 2012
230. **Quantifying Regional Economic Impacts of CO₂ Intensity Targets in China** *Zhang et al.* September 2012
231. **The Future Energy and GHG Emissions Impact of Alternative Personal Transportation Pathways in China** *Kishimoto et al.* September 2012
232. **Will Economic Restructuring in China Reduce Trade-Embodied CO₂ Emissions?** *Qi et al.* October 2012
233. **Climate Co-benefits of Tighter SO₂ and NO_x Regulations in China** *Nam et al.* October 2012
234. **Shale Gas Production: Potential versus Actual GHG Emissions** *O'Sullivan and Paltsev* November 2012
235. **Non-Nuclear, Low-Carbon, or Both? The Case of Taiwan** *Chen* December 2012
236. **Modeling Water Resource Systems under Climate Change: IGSM-WRS** *Strzepek et al.* December 2012